OXFORD

Cerebral Cortex, 2023, **33**, 3319–3349
https://doi.org/10.1093/cercor/bhac276
Advance access publication date 14 July 2022
Original Article

Multiple cortical visual streams in humans

Edmund T. Rolls [1,2,3,*], Gustavo Deco[4,5,6], Chu-Chung Huang[7,8], Jianfeng Feng[2,3]

[1]Oxford Centre for Computational Neuroscience, Oxford, United Kingdom,
[2]Department of Computer Science, University of Warwick, Coventry CV4 7AL, United Kingdom,
[3]Institute of Science and Technology for Brain Inspired Intelligence, Fudan University, Shanghai 200403, China,
[4]Computational Neuroscience Group, Department of Information and Communication Technologies, Center for Brain and Cognition, Universitat Pompeu Fabra, Roc Boronat 138, Barcelona 08018, Spain,
[5]Brain and Cognition, Pompeu Fabra University, Barcelona 08018, Spain,
[6]Institució Catalana de la Recerca i Estudis Avançats (ICREA), Universitat Pompeu Fabra, Passeig Lluís Companys 23, Barcelona 08010, Spain,
[7]Shanghai Key Laboratory of Brain Functional Genomics (Ministry of Education), Institute of Brain and Education Innovation, School of Psychology and Cognitive Science, East China Normal University, Shanghai 200602, China,
[8]Shanghai Center for Brain Science and Brain-Inspired Technology, Shanghai 200602, China

*Corresponding author: Department of Computer Science, University of Warwick, Coventry CV4 7AL, United Kingdom. Email: Edmund.Rolls@oxcns.org

The effective connectivity between 55 visual cortical regions and 360 cortical regions was measured in 171 HCP participants using the HCP-MMP atlas, and complemented with functional connectivity and diffusion tractography. A Ventrolateral Visual "What" Stream for object and face recognition projects hierarchically to the inferior temporal visual cortex, which projects to the orbitofrontal cortex for reward value and emotion, and to the hippocampal memory system. A Ventromedial Visual "Where" Stream for scene representations connects to the parahippocampal gyrus and hippocampus. An Inferior STS (superior temporal sulcus) cortex Semantic Stream receives from the Ventrolateral Visual Stream, from visual inferior parietal PGi, and from the ventromedial-prefrontal reward system and connects to language systems. A Dorsal Visual Stream connects via V2 and V3A to MT+ Complex regions (including MT and MST), which connect to intraparietal regions (including LIP, VIP and MIP) involved in visual motion and actions in space. It performs coordinate transforms for idiothetic update of Ventromedial Stream scene representations. A Superior STS cortex Semantic Stream receives visual inputs from the Inferior STS Visual Stream, PGi, and STV, and auditory inputs from A5, is activated by face expression, motion and vocalization, and is important in social behaviour, and connects to language systems.

Key words: effective connectivity; visual cortex; functional connectivity; diffusion tractography; what and where visual systems; spatial view.

Introduction

Given the great development and heterogeneity of functions of different parts of the human visual system (Vul et al. 2012; Deen et al. 2015; Weiner and Grill-Spector 2015; Isik et al. 2017; Weiner et al. 2017; Rajalingham et al. 2018; Sulpizio et al. 2020; Vanni et al. 2020; Caffarra et al. 2021; Natu et al. 2021; Orban et al. 2021; Pitcher and Ungerleider 2021) and related foundational studies in macaques (Perrett et al. 1982; Hasselmo, Rolls, Baylis 1989a; Hasselmo, Rolls, Baylis, Nalwa 1989b; Felleman and Van Essen 1991; Rolls 2000; Rolls and Treves 2011; Markov et al. 2014; Tsao 2014; Freiwald 2020; Rolls 2021a), and the importance for understanding brain computations of evidence about the connectivity of different visual cortical regions (Rolls 2000; Rajalingham et al. 2018; Zhuang et al. 2021; Rolls 2021a, 2021b), the aim of the present investigation is to advance understanding of the connections and connectivity of the human cortical visual systems.

To do this, we measured with Human Connectome Project data (Glasser, Smith, et al. 2016b) the direct connections between cortical regions using diffusion tractography; the functional connectivity between cortical regions using the correlation between the BOLD signals in resting state fMRI, which provides evidence about the strength of interactions; and the effective connectivity, which provides evidence about the strength and direction of the causal connectivity between pairs of hundreds of cortical regions with a new Hopf algorithm (Rolls 2022a; Rolls, Deco, et al. 2022c, 2022d, 2022e). These measures were made between the 360 cortical regions in the Human Connectome Project multimodal parcellation atlas (HCP-MMP) (Glasser, Coalson, et al. 2016a). The HCP-MMP atlas provides the most detailed parcellation of the human cortical areas that we know, in that its 360 regions are defined using a combination of structural measures (cortical thickness and cortical myelin content), functional connectivity, and task-related fMRI (Glasser, Coalson, et al. 2016a). This parcellation is the parcellation of choice for the cerebral cortex because it is based on multimodal information (Glasser, Coalson, et al. 2016a) with the definition and boundaries set out in their Glasser_2016_SuppNeuroanatomy.pdf, and it is being used as the basis for many new investigations of brain function and connectivity, which can all be cast in the same framework (Colclough et al. 2017;

Received: May 10, 2022. **Revised:** June 16, 2022. **Accepted:** June 17, 2022

Van Essen and Glasser 2018; Sulpizio et al. 2020; Yokoyama et al. 2021; Rolls 2022a; Rolls, Deco, et al. 2022c, 2022d, 2022e; Rolls, Wirth, et al. 2022f). This approach provides better categorization of cortical areas than does for example functional connectivity alone (Power et al. 2011). A summary of the boundaries, tractography, functional connectivity and task-related activations of visual cortical areas using the HCP-MMP atlas is available elsewhere (Glasser, Coalson, et al. 2016a; Baker, Burks, Briggs, Conner, et al. 2018a; Baker, Burks, Briggs, Milton, et al. 2018b), but the effective connectivity, tractography, and functional connectivity analyses described here are new, and further are presented in quantitative form using connectivity matrices for all 360 cortical areas.

Previous understanding of cortical visual information streams has been founded on research in non-human primates (Felleman and Van Essen 1991; Ungerleider 1995; Kravitz et al. 2013), supplemented by activation and functional connectivity studies in humans with dorsal and ventral streams identified (Ungerleider and Haxby 1994; Van Essen and Glasser 2018), and complemented by neuropsychological studies (Milner and Goodale 1995; Milner 2017; Gallivan and Goodale 2018). The discovery of a third visual processing stream in the cortex in the superior temporal sulcus for face and object motion and face expression with auditory inputs and important in social behavior (Baylis et al. 1987; Hasselmo, Rolls, Baylis 1989a; Hasselmo, Rolls, Baylis, Nalwa 1989b) has received support more recently (Pitcher and Ungerleider 2021). The present research goes beyond this previous research by estimating causal connectivity between 55 visual cortical regions in the human brain with a multimodal atlas with 360 cortical areas. Strengths of this investigation are that it utilized this HCP-MMP atlas (Glasser, Coalson, et al. 2016a); HCP data from the same set of 171 participants imaged at 7T (Glasser, Smith, et al. 2016b) in whom we could calculate the connections, functional connectivity, and effective connectivity; and that it utilized a method for effective connectivity measurement between all 360 cortical regions investigated here. The Hopf effective connectivity algorithm is important for helping to understand the operation of the computational system, for it is calculated using time delays in the signals between 360 or more cortical regions (Rolls 2022a; Rolls, Deco, et al. 2022c, 2022d, 2022e), and the use of time is an important component in the approach to causality (Rolls 2021c). These methods allowed us to delineate 5 cortical visual streams in humans, as described here. We hope that future research using the same brain atlas (Glasser, Coalson, et al. 2016a; Huang et al. 2022) will benefit from the human visual cortical connectome described here.

Methods

Participants and data acquisition

Multiband 7T resting state functional magnetic resonance images (rs-fMRI) of 184 individuals were obtained from the publicly available S1200 release (last updated: April 2018) of the Human Connectome Project (HCP) (Van Essen et al. 2013). Individual written informed content was obtained from each participant, and the scanning protocol was approved by the Institutional Review Board of Washington University in St. Louis, MO, USA (IRB #201204036).

Multimodal imaging was performed in a Siemens Magnetom 7T housed at the Center for Magnetic Resonance (CMRR) at the University of Minnesota in Minneapolis. For each participant, a total of four sessions of rs-fMRI were acquired, with oblique axial acquisitions alternated between phase encoding in a posterior-to-anterior (PA) direction in sessions 1 and 3, and an anterior-to-posterior (AP) phase encoding direction in sessions 2 and 4. Specifically, each rs-fMRI session was acquired using a multiband gradient-echo EPI imaging sequence. The following parameters were used: TR = 1,000 ms, TE = 22.2 ms, flip angle = 45°, field of view = 208 × 208, matrix = 130 × 130, 85 slices, voxel size = 1.6 × 1.6 × 1.6 mm^3, multiband factor = 5. The total scanning time for the rs-fMRI protocol was approximately 16 min with 900 volumes. Further details of the 7T rs-fMRI acquisition protocols are given in the HCP reference manual (https://humanconnectome.org/storage/app/media/documentation/s1200/HCP_S1200_Release_Reference_Manual.pdf).

The current investigation was designed to complement investigations of effective and functional connectivity and diffusion tractography of the hippocampus (Huang et al. 2021; Ma et al. 2022; Rolls, Deco, et al. 2022d), posterior cingulate cortex (Rolls, Wirth, et al. 2022f), parietal cortex (Rolls, Deco, et al. 2022a), orbitofrontal, ventromedial prefrontal, and anterior cingulate cortex (Rolls, Deco, et al. 2022e), and language cortical regions (Rolls, Deco, et al. 2022c), and so the same 171 participants with data for the first session of rs-fMRI at 7T were used for the analyses described here (age 22–36 years, 66 males).

Data preprocessing

The preprocessing was performed by the HCP as described in Glasser et al. (2013), based on the updated 7T data pipeline (v3.21.0, https://github.com/Washington-University/HCPpipelines), including gradient distortion correction, head motion correction, image distortion correction, spatial transformation to the Montreal Neurological Institute space using one step spline resampling from the original functional images followed by intensity normalization. In addition, the HCP took an approach using ICA (FSL's MELODIC) combined with a more automated component classifier referred to as FIX (FMRIB's ICA-based X-noisifier) to remove non-neural spatiotemporal artifact (Smith et al. 2013; Griffanti et al. 2014; Salimi-Khorshidi et al. 2014). This step also used 24 confound timeseries derived from the motion estimation (6 rigid-body parameter timeseries, their backwards-looking temporal derivatives, plus all 12 resulting regressors squared (Satterthwaite et al. 2013) to minimize noise in the data. The preprocessing performed

by the HCP also included boundary-based registration between EPI and T1w images, and brain masking based on FreeSurfer segmentation. The "minimally preprocessed" rsfMRI data provided by the HCP 1200 release (rfMRI*hp2000_clean.dtseries) was used in this investigation. The preprocessed data are in the HCP grayordinates standard space and are made available in a surface-based CIFTI file for each participant. With the MATLAB script (cifti toolbox: https://github.com/Washington-University/cifti-matlab), we extracted and averaged the cleaned timeseries of all the grayordinates in each region of the HCP-MMP 1.0 atlas (Glasser, Coalson, et al. 2016a), which is a group-based parcellation defined in the HCP grayordinate standard space having 180 cortical regions per hemisphere, and is a surface-based atlas provided in CIFTI format. The timeseries were detrended, and temporally filtered with a second order Butterworth filter set to 0.008–0.08 Hz.

Brain atlas and region selection

To construct the effective connectivity for the regions of interest in this investigation with other parts of the human brain, we utilized the 7T resting state fMRI data the HCP, and parcellated this with the surface based HCP-MMP atlas, which has 360 cortical regions (Glasser, Coalson, et al. 2016a). We were able to use the same 171 participants for whom we also had performed diffusion tractography, as described in detail (Huang et al. 2021). The brain regions in this atlas (Glasser, Coalson, et al. 2016a) are shown in Figs. 6–10 and Fig. S1, and a list of the cortical regions in this atlas and the divisions into which they are placed is provided in Table S1 in the reordered form used in the extended volumetric HCPex atlas (Huang et al. 2022).

The 55 visual cortical regions selected for connectivity analysis here were as follows, in the HCP-MMP division indicated where relevant. These 55 regions were selected because they are primarily of the cortical regions in the divisions listed below which are the main visual cortical divisions in the HCP-MMP atlas (Glasser, Coalson, et al. 2016a). Some additional regions with visual responses such as the eye fields and the parahippocampal gyrus regions were also included to provide evidence about how visual inputs reach these regions, but most of the hippocampal system was not included here as it has been considered elsewhere (Huang et al. 2021; Ma et al. 2022; Rolls, Deco, et al. 2022d). Some other visual cortical regions in other divisions of the HCP-MMP atlas including ProS, POS1-2, and DVT have been included in analyses of the cortical regions in the Posterior Cingulate division of the HCP-MMP atlas (Rolls, Wirth, et al. 2022f). The connectivity of Area 7 parietal cortex regions has been described in an analysis of the connectivity of the parietal cortex (Rolls, Deco, et al. 2022a). It is noted that the HCP-MMP atlas sometimes uses dorsal vs ventral as descriptors following nomenclature in non-human primates, and that these correspond to superior and inferior in humans. For those becoming familiar with the HCP-MMP atlas, in the name of a cortical region typically a = anterior, p = posterior, d = dorsal (i.e. superior in the human brain), v = ventral (i.e. inferior in the human brain), m = medial, l or L = lateral, T = temporal, P = parietal, and V = visual. It must also be noted that some of the names used in the HCP-MMP atlas utilize the name of the corresponding region in macaques, but in humans the cortical region may not be topologically in the same place (e.g. sulcus) as in macaques.

Primary Visual division: Primary visual cortex V1;

Early Visual cortical division: V2, V3, V4;

Dorsal Stream Visual Division: Intraparietal Sulcus Area 1 IPS1, V3A, V3B, V6, V6A and V7;

Ventral Stream Visual Division: Fusiform face Complex FFC, Posterior Inferotemporal complex PIT, V8, Ventromedial Visual Areas 1–3 VMV1-VMV3, Ventral Visual Complex VVC;

MT+ complex division: FST, Lateral Occipital Areas 1–3 LO1-LO3, Medial Superior Temporal Areas MST, Middle Temporal Area MT, PH, V3CD and V4t (it is noted that an MT cluster has been described that includes FST, MST, MT, and v4t (Kolster et al. 2010); but that the MT+ complex division of the HCP-MMP includes more cortical regions as just specified (Glasser, Coalson, et al. 2016a));

Eye Field regions: Supplementary and Cingulate Eye Field SCEF, Frontal Eye Fields FEF, Premotor Eye Fields PEF;

Superior temporal Sulcus regions with visual responses: STGa, STS dorsal anterior STSda, STS dorsal posterior STSdp, STS ventral anterior STSva, STS ventral posterior STSvp;

Parahippocampal gyrus regions with visual responses: TF, Parahippocampal area 1–3 PHA1-PHA3 (which correspond to macaque TH);

Lateral Temporal division: PHT, TE1 anterior TE1a, TE1 middle TE1m; TE1 posterior TE1p, TE2 anterior TE2a, TE2 posterior TE2p, temporal pole TG dorsal TGd, temporal pole ventral TGv;

Intraparietal sulcus regions in the Superior Parietal division: Anterior IntraParietal Area AIP, Lateral Intraparietal dorsal region LIPd, Lateral Intraparietal ventral region LIPv, Medial Intraparietal area MIP, and Ventral IntraParietal complex VIP. Intraparietal area 0—Intraparietal Area 2 IP0—IP2 from the inferior parietal division are also included for completeness.

It is noted that other visual parts of the superior and inferior parietal cortex including the area 7 regions and PGi, PGp PGs and PFm are considered in a separate paper on the parietal cortex connectome (Rolls, Deco, et al. 2022a), but their connectivities are referred to here where appropriate. Cross-reference is also made to analyses of connectivity that complement the results described here in that they use the same methods and are from the same HCP participants so can be directly compared, for the orbitofrontal cortex, ventromedial prefrontal cortex (vmPFC), and anterior cingulate cortex (Rolls, Deco, et al. 2022e); for the hippocampal memory system (Huang et al. 2021; Ma et al. 2022; Rolls, Deco, et al. 2022d); for the posterior parietal cortex (Rolls, Deco, et al. 2022a); for

the posterior cingulate cortex (Rolls, Wirth, et al. 2022f); and for cortical regions involved in language (Rolls, Deco, et al. 2022c).

Measurement of effective connectivity

Effective connectivity measures the effect of one brain region on another, and utilizes differences detected at different times in the signals in each connected pair of brain regions to infer effects of one brain region on another. One such approach is dynamic causal modeling, but it applies most easily to activation studies, and is typically limited to measuring the effective connectivity between just a few brain areas (Friston 2009; Valdes-Sosa et al. 2011; Bajaj et al. 2016), though there have been moves to extend it to resting state studies and more brain areas (Frassle et al. 2017; Razi et al. 2017). The method used here (see Rolls, Deco, et al. 2022d, 2022e) was developed from a Hopf algorithm to enable measurement of effective connectivity between many brain areas, described by Deco et al. (2019). A principle is that the functional connectivity is measured at time t and time $t+$ tau, where tau is typically 2 s to take into account the time within which a change in the BOLD signal can occur, and that tau should be short to capture causality, and then the effective connectivity model is trained by error correction until it can generate the functional connectivity matrices at time t and time t + tau. Further details of the algorithm, and the development that enabled it to measure the effective connectivity in each direction, are described next and in more detail in the Supplementary Material.

To infer the effective connectivity, we use a whole-brain model that allows us to simulate the BOLD activity across all brain regions and time. We use the so-called Hopf computational model, which integrates the dynamics of Stuart-Landau oscillators, expressing the activity of each brain region, by the underlying anatomical connectivity (Deco, Kringelbach, et al. 2017b). As mentioned above, we include in the model 360 cortical brain areas (Huang et al. 2022). The local dynamics of each brain area (node) is given by Stuart-Landau oscillators, which expresses the normal form of a supercritical Hopf bifurcation, describing the transition from noisy to oscillatory dynamics (Kuznetsov 2013). During the last years, numerous studies were able to show how the Hopf whole-brain model successfully simulates empirical electrophysiology (Freyer et al. 2011; Freyer et al. 2012), MEG (Deco, Cabral, et al. 2017a) and fMRI (Kringelbach et al. 2015; Deco, Kringelbach, et al. 2017b; Kringelbach and Deco 2020).

The Hopf whole-brain model can be expressed mathematically as follows:

$$\frac{dx_i}{dt} = \overbrace{\left[a_i - x_i^2 - y_i^2\right]x_i - \omega_i y_i}^{\text{Local Dynamics}} + \overbrace{G\sum_{j=1}^{N} C_{ij}\left(x_j - x_i\right)}^{\text{Coupling}} + \overbrace{\beta\eta_i(t)}^{\text{Gaussian Noise}} \quad (1)$$

$$\frac{dy_i}{dt} = \left[a_i - x_i^2 - y_i^2\right]y_i + \omega_i x_i + G\sum_{j=1}^{N} C_{ij}\left(y_j - y_i\right) + \beta\eta_i(t) \quad (2)$$

Equations (1) and (2) describe the coupling of Stuart-Landau oscillators through an effective connectivity matrix C. The $x_i(t)$ term represents the simulated BOLD signal data of brain area i. The values of $y_i(t)$ are relevant to the dynamics of the system but are not part of the information read out from the system. In these equations, $\eta_i(t)$ provides additive Gaussian noise with standard deviation β. The Stuart-Landau oscillators for each brain area i express a Hopf normal form that has a supercritical bifurcation at $a_i = 0$, so that if $a_i > 0$ the system has a stable limit cycle with frequency $f_i = \omega_i/2\pi$ (where ω_i is the angular velocity); and when $a_i < 0$ the system has a stable fixed point representing a low activity noisy state. The intrinsic frequency f_i of each Stuart-Landau oscillator corresponding to a brain area is in the 0.008–0.08 Hz band ($i = 1, \ldots, 360$). The intrinsic frequencies are fitted from the data, as given by the averaged peak frequency of the narrowband BOLD signals of each brain region. The coupling term representing the input received in node i from every other node j, is weighted by the corresponding effective connectivity C_{ij}. The coupling is the canonical diffusive coupling, which approximates the simplest (linear) part of a general coupling function. G denotes the global coupling weight, scaling equally the total input received in each brain area. While the oscillators are weakly coupled, the periodic orbit of the uncoupled oscillators is preserved. Details are provided in the Supplementary Material.

The effective connectivity matrix is derived by optimizing the conductivity of each existing anatomical connection as specified by the Structural Connectivity matrix (measured with tractography (Huang et al. 2021)) in order to fit the empirical functional connectivity (FC) pairs and the lagged FC^{tau} pairs. By this, we are able to infer a non-symmetric Effective Connectivity matrix (see Gilson et al. (2016)). Note that FC^{tau}, i.e. the lagged functional connectivity between pairs, lagged at *tau* s, breaks the symmetry and thus is fundamental for our purpose. Specifically, we compute the distance between the model FC simulated from the current estimate of the effective connectivity and the empirical data FC^{emp}, as well as the simulated model FC^{tau} and empirical data FC^{tau_emp} and adjust each effective connection (entry in the effective connectivity matrix) separately with a gradient-descent approach. The model is run repeatedly with the updated effective connectivity until the fit converges towards a stable value.

We start with the anatomical connectivity obtained with probabilistic tractography from dMRI (or from an initial zero C matrix as described in the Supplementary Material) and use the following procedure to update each entry C_{ij}in the effective connectivity matrix

$$C_{ij} = C_{ij} + \varepsilon\left(FC_{ij}^{emp} - FC_{ij} + FC_{ij}^{tau\_emp} - FC_{ij}^{tau}\right) \quad (3)$$

where ϵ is a learning rate constant, and i and j are the nodes. When updating each connection if the initial matrix is a dMRI structural connection matrix (see Supplementary Material), the corresponding link to the same brain regions in the opposite hemisphere is also updated, as contralateral connections are not revealed well by dMRI. The convergence of the algorithm is illustrated by Rolls, Deco, et al. (2022d), and the utility of the algorithm was validated as described below.

For the implementation, we set tau to be 2 s, selecting the appropriate number of TRs to achieve this. The maximum effective connectivity was set to a value of 0.2, and was found between V1L and V1R.

Effective connectome

Whole-brain effective connectivity (EC) analysis was performed between the 55 visual cortical regions described above (see Figs. 6–10 and Fig. S1) and the 360 regions defined in the surface-based HCP-MMP atlas (Glasser, Coalson, et al. 2016a) in their reordered form provided in Table S1, described in the Supplementary Material, and used in the volumetric extended HCPex atlas (Huang et al. 2022). This EC was computed for all 171 participants. The effective connectivity algorithm was run until it had reached the maximal value for the correspondence between the simulated and empirical functional connectivity matrices at time t and $t+$ tau (see Supplementary Material). The effective connectivity calculated was checked and validated in a number of ways described in the Supplementary Material.

To test whether the vectors of effective connectivities of each of the 55 visual cortex regions with the 180 areas in the left hemisphere of the modified HCP atlas were significantly different, the interaction term was calculated for each pair of the 55 visual cortex regions effective connectivity vectors in separate two-way ANOVAs (each 2×180) across the 171 participants, and Bonferroni correction for multiple comparisons was applied. The results were checked with the non-parametric Scheirer-Rey-Hare test (Scheirer et al. 1976; Sinha 2022).

Functional connectivity

For comparison with the effective connectivity, the functional connectivity was also measured at 7T with the identical set of participants, data, and filtering of 0.008–0.08 Hz. The functional connectivity was measured by the Pearson correlation between the BOLD signal timeseries for each pair of brain regions, and is in fact the FC^{emp} referred to above. A threshold of 0.4 is used for the presentation of the findings in Fig. 4, for this sets the sparseness of what is shown to a level commensurate with the effective connectivity, to facilitate comparison between the functional and the effective connectivity. The functional connectivity can provide evidence that may relate to interactions between brain regions, while providing no evidence about causal direction-specific effects. A high functional connectivity may in this scenario thus reflect strong physiological interactions between areas, and provides a different type of evidence to effective connectivity. The effective connectivity is non-linearly related to the functional connectivity, with effective connectivities being identified (i.e. greater than zero) only for the links with relatively high functional connectivity.

Connections shown with diffusion tractography

Diffusion tractography can provide evidence about fiber pathways linking different brain regions with a method that is completely different to the ways in which effective and functional connectivity are measured, so is included here to provide complementary and supporting evidence to the effective connectivity. Diffusion tractography shows only direct connections, so comparison with effective connectivity can help to suggest which effective connectivities may be mediated directly or indirectly. Diffusion tractography does not provide evidence about the direction of connections. Diffusion tractography was performed on the same 171 HCP participants imaged at 7T with methods described in detail elsewhere (Huang et al. 2021). The major parameters were: 1.05 mm isotropic voxels; a 2-shell acquisition scheme with b-values = 1,000, 2,000 s/mm^2, repetition time/echo time = 7,000/71 ms, 65 unique diffusion gradient directions and 6 b0 images obtained for each phase encoding direction pair (AP and PA pairs). Pre-processing steps included distortion correction, eddy-current correction, motion correction, and gradient non-linearity correction. In brief, whole brain tractography was reconstructed for each subject in native space. To improve the tractography termination accuracy in GM, MRtrix3's 5ttgen command was used to generate multi-tissue segment images (5tt) using T1 images, the segmented tissues were then co-registered with the b0 image in diffusion space. For multi-shell data, tissue response functions in GM, WM, and CSF were estimated by the MRtrix3' dwi2response function with the Dhollander algorithm (Dhollander et al. 2016). A Multi-Shell Multi-Tissue Constrained Spherical Deconvolution (MSMT-CSD) model with lmax = 8 and prior co-registered 5tt image was used on the preprocessed multi-shell DWI data to obtain the fiber orientation distribution (FOD) function (Smith 2002; Jeurissen et al. 2014). Based on the voxel-wise fiber orientation distribution, anatomically-constrained tractography (ACT) using the using the probabilistic tracking algorithm: iFOD2 (second order integration based on FOD) with dynamic seeding was applied to generate the initial tractogram (1 million streamlines with maximum tract length = 250 mm and minimal tract length = 5 mm). To quantify the number of streamlines connecting pairs of regions, the updated version of the spherical-deconvolution informed filtering of the tractograms (SIFT2) method was applied, which

provides more biologically meaningful estimates of structural connection density (Smith et al. 2015).

The results for the tractography are shown in Fig. 5 as the number of streamlines between areas with a threshold applied of 10 to reduce the risk of occasional noise-related observations. The highest level in the color bar was set to 1,000 streamlines between a pair of cortical regions in order to show graded values for a number of links, but the value for the number of streamlines between V1 and V2 was in fact higher at close to 10,000. The term "connections" is used when referring to what is shown with diffusion tractography, and connectivity when referring to effective or functional connectivity.

Results

Overview: effective connectivity, functional connectivity, and diffusion tractography

The effective connectivities to the 55 visual cortical regions from other cortical regions in the left hemisphere are shown in Fig. 1. The effective connectivities *from* the 55 visual cortical regions to other cortical regions in the left hemisphere are shown in Fig. 2. The vectors of effective connectivities of each of the 55 visual cortical regions with the 180 regions in the left hemisphere of the HCP-MMP atlas were all significantly different from each other. (Across the 171 participants the interaction term in separate two-way ANOVAs for the comparisons between the effective connectivity of every pair of the 55 ROIs after Bonferroni correction for multiple comparisons were all $P < 10^{-90}$. The results were confirmed with the non-parametric Scheirer-Rey-Hare test (Scheirer et al. 1976; Sinha 2022).) The connectivity of each of the cortical divisions set out above are considered division by division in the Results, as this helps closely related regions to be described together. The effective connectivities described in the text are the stronger ones, typically >0.01, but all of those greater than 0 are shown in the figures. The functional implications of the results described next are considered in the Discussion.

Primary Visual division: Primary visual cortex V1.

The strongest effective connectivity of V1 is with contralateral V1, and that is the highest effective connectivity in the brain (and was set to 0.2). Within a hemisphere, the highest effective connectivity of V1 is to V2 with a value of 0.15 (Fig. 1 and Fig. S1-6), and as this is the highest connectivity within a hemisphere, the effective connectivity matrices shown here are set to show a maximum value of 0.15. V1 has lower effective connectivity to V3, and lower still to V4 (Fig. 1 and Fig. S1-6). In terms of backprojections, V2 to V1 is lower than the forward connectivity, and V4 to V3 is lower than the forward connectivity, but V3 to V2 does not follow the more general rule. This more general rule is evident over many visual cortical regions, as shown by the generally positive differences in the forward direction in the connectivities below the diagonal in the upper left of Fig. 3, and generally negative differences for the forward direction in the connectivities above the diagonal in the upper right of Fig. 3.

V1 does also have clear effective connectivity to V3A, V6, V8, and VMV1 (Fig. 1 and Fig. S1-6).

The functional connectivity thresholded at 0.4 is less selective in what it shows (Fig. 4) than the effective connectivity (Figs. 1 and 2), and of course provides no evidence about direction as functional connectivity is measured by a correlation in the BOLD signal of each pair of brain regions.

The diffusion tractography (Fig. 5) is also less selective than the effective connectivity.

Early visual cortical division: V2, V3, V4

The effective connectivity provides evidence for hierarchical organization in humans, with strong connections from V1 to V2, from V2 to V3, and from V3 to V4 (Fig. 1 and Fig. S1-6). Moreover, this is the forward direction, in that in general the effective connectivity is weaker in the reverse direction (Figs. 1, 3, and Fig. S1-6).

In addition, V2 has some (forward) effective connectivity with V4, V3A, V6, V8, and VMV1. Some of these effects might not be monosynaptic, and this is considered in the Discussion.

V3 has in addition to effective connectivity to V4, also connectivity to V3A, V3B, PIT, V8, VMV3, and LO2.

V4 has effective connectivity to V3B, PIT, V8, VMV3, LO1, LO2, and V3CD.

As shown in Fig. 3, most of the connectivities are stronger in the direction described here, and so are probably forward projections.

Dorsal stream visual division: IPS1 (Intraparietal Sulcus Area 1), V3A, V3B, V6, V6A, and V7.

IPS1 receives from V3B, V6A, V7, PH, FST, LO1, LO2, PH, V3CD, LIPV, MIP, VIP, and IP0 (Figs. 1, 2 and Fig. S1-6). Most of these connectivities apart from LO1 are relatively similar in strength in both directions. IPS1 thus is a key region in the dorsal visual stream, with connectivity that includes intraparietal cortical regions. Its connectivity with contralateral IPS1 is high (0.1).

V3A receives inputs from V1, V2, V3, V4, V3B, V6, and V7. Most of these effective connectivities are substantial in both directions except that V1 projects more strongly to V3A than vice versa. Effective connectivities from V3A are stronger in the direction to VMV1, VMV2, VMV3, LO1, LO3, MST, MT, V3CD, and V4t (Figs. 1–3). V3A is thus a key region in the dorsal visual stream, with connectivity from early visual cortical regions V1-V4, and outputs directed to dorsal stream regions that are motion-sensitive including MT, MST, and also are directed to VMV1-VMV3.

V3B receives inputs from V2, V3, and V4 (which are stronger in that direction); and from IPS1, V3A, V6A, V7, V8, LO1, LO2, V3CD, VIP, and IP0 (which are more similar in each direction). V3A has stronger effective connectivity than the reverse to VMV2, VMV3, VVC, and LIPv (Figs. 1–3). V3B may thus be a region that

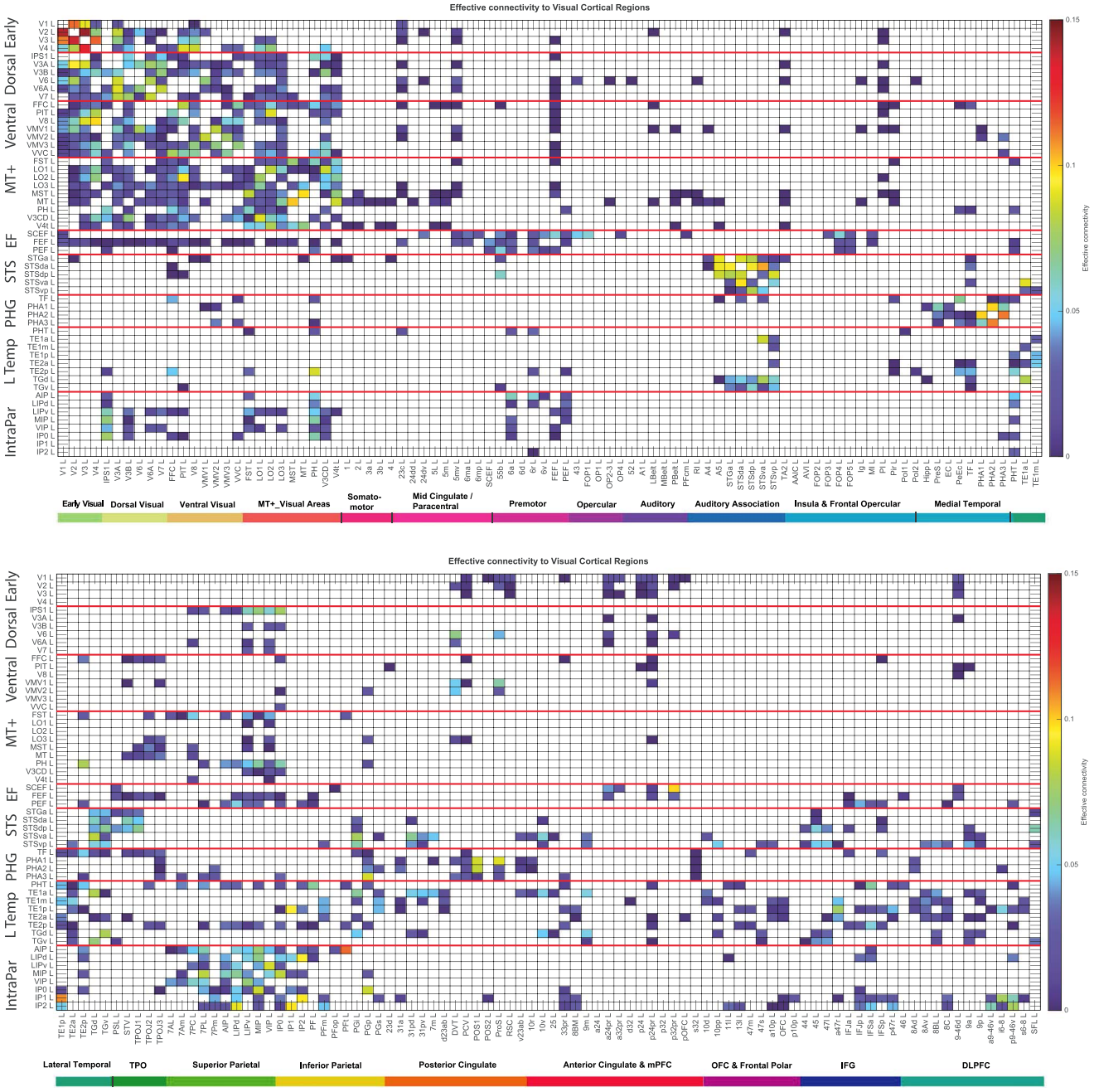

Fig. 1. Effective connectivity *TO* visual cortical regions (the rows) *FROM* 180 cortical areas (the columns) in the left hemisphere. The effective connectivity is read from column to row. Effective connectivities of 0 are shown as blank. All effective connectivity maps are scaled to show 0.15 as the maximum, as this is the highest effective connectivity found between this set of brain regions. The effective connectivity algorithm for the whole brain is set to have a maximum of 0.2, and this was for connectivity between V1L and V1R. The effective connectivity for the first set of cortical regions is shown in the top panel; and for the second set of regions in the lower panel. Abbreviations: See Table S1. The groups of visual cortex regions are separated by red lines. Group 1 (top) Early Visual division of the HCP-MMP atlas (labeled on the left Early); Group 2 Dorsal Visual division (Dorsal); Group 3 Ventral Visual division (Ventral); Group 4 MT+ division (MT+); Group 5 Eye Field regions (EF); Group 6 Superior Temporal Sulcus regions (STS); Group 7 Medial Temporal Regions (PHG, parahippocampal gyrus); Group 8 Lateral Temporal division including the Temporal Pole (L Temp); Group 9 Intraparietal sulcus regions (IntraPar). The colored labeled bars show the cortical divisions in the HCP-MMP atlas (Glasser, Coalson, et al. 2016a). The order of the cortical regions is that in Huang, Rolls et al (2022).

receives from early cortical visual regions apart from V1, and has connectivity with regions such as IPS1 and dorsal stream areas reaching into intraparietal visual cortical regions that have visual motion-responsive activity.

V6 receives inputs from V1, V2, and V3 (in that direction), and has more similar connectivity in both directions with V3A, V6A, VMV1, VMV2, LO3. It has connections that are more in the direction to MT. However, V6 is different to the visual areas considered so far, in that it has some (typically weak) effective connectivity mainly with somatosensory (3a, 5mv, 43, OP2–3, OP4) and premotor or related regions (posterior cingulate DVT and PRoS, and supracallosal anterior cingulate a24pr,

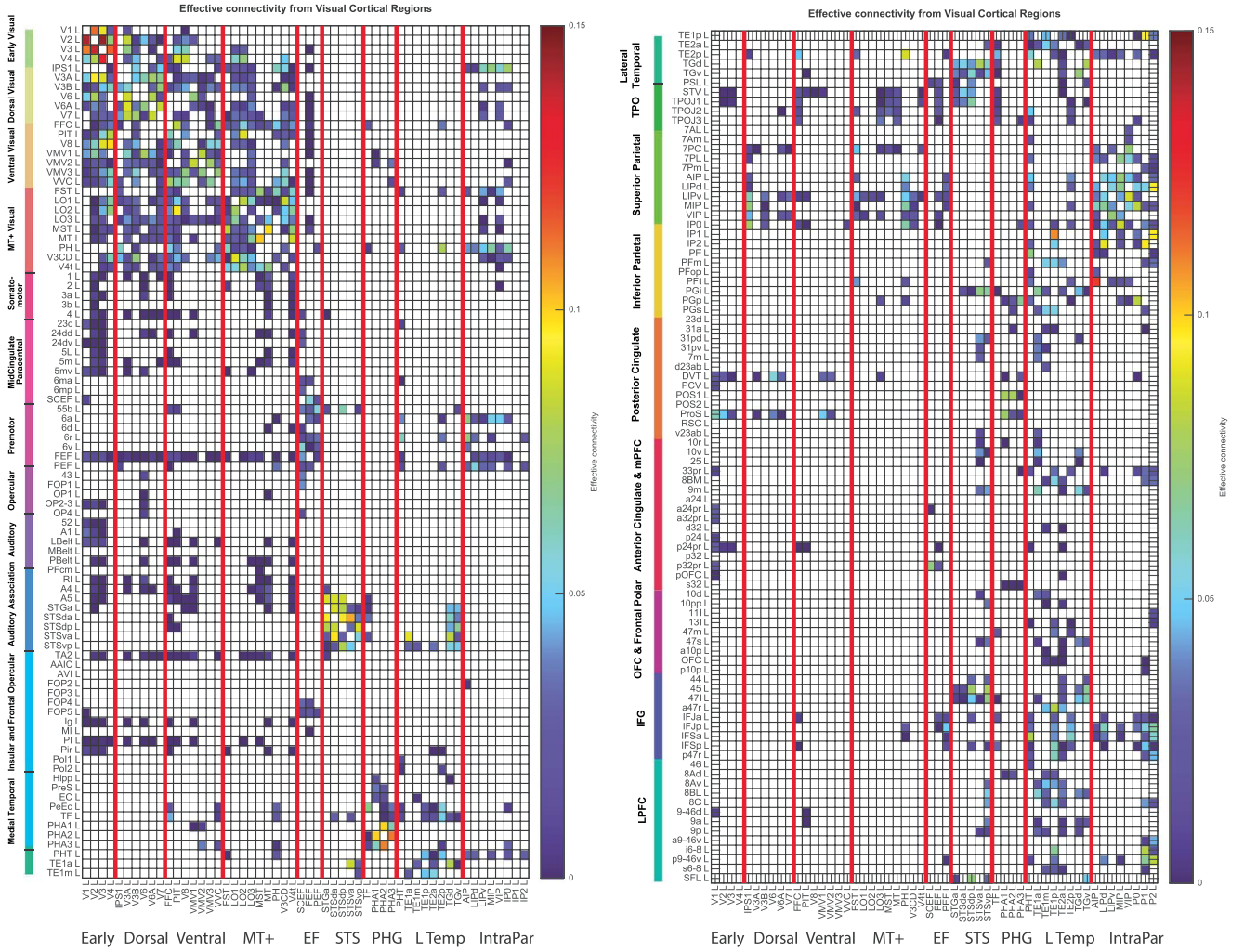

Fig. 2. Effective connectivity *FROM* the visual cortical regions *TO* 180 cortical areas in the left hemisphere. The effective connectivity is read from column to row. Effective connectivities of 0 are shown as blank. Abbreviations: See Table S1. The groups of visual cortex areas are separated by red lines.

p24pr, p32pr) the connectivities of which are described elsewhere but which include somatosensory inputs (Rolls, Deco, et al. 2022e; Rolls, Wirth, et al. 2022f).

V6A receives inputs from V2 and V3 (in that direction), and has more similar connectivity in both directions with IPS1, V3A, V3B, V6, V7, LO3, V4t, and VIP. V6A has connectivity directed to VMV1-VMV3, MST, MT, and 7PC. V6A is thus a dorsal stream region with connectivity with some MT+ complex regions leading to parietal visual areas, and also with some medial temporal visual regions (VMV1–3). There is also connectivity with the dorsal visual transitional (DVT) region in the posterior cingulate division (Rolls, Wirth, et al. 2022f).

V7 receives inputs from V2, V3, and V4 (in that direction), and has more similar connectivity in both directions with IPS1, V3A, V3B, V6A, LO1-LO3, V3CD, V4t, LIPv, and VIP. It has connectivity primarily in the direction towards VMV1, VMV3, and VVC. Its onwards connectivity is thus especially with intraparietal motion areas, and with some medial temporal lobe regions (VMV and VVC).

Ventral Stream Visual Division: Fusiform Face Complex FFC, Posterior Inferotemporal complex PIT, V8, Ventromedial Visual Areas 1-3 VMV1-VMV3, Ventral Visual Complex VVC.

The FFC receives from V3 and V4, has strong effective connectivity with PIT and V8 and VVC, and also has moderate connectivity with many MT+ complex regions including FST, LO1-LO3, MST, MT, PHV3CD, and V4t. It thus combines ventral stream information (PIT, V8, and VVC) with motion information from the MT+ complex. It also has connectivity directed to the inferior temporal visual cortex TE2p, to the hippocampal system (perirhinal cortex PeEc and "what" part of the parahippocampal gyrus TF (Rolls, Deco, et al. 2022d)), and to temporo-parieto-occipital regions TPOJ1-TPOJ3 and STV implicated in language (Rolls, Deco, et al. 2022c) (Figs. 1–3).

PIT is connected with V3 and V4 (and less with V2), and connects to V3B, FFC, V8, VMV3, VVC, a number of MT+ Complex regions (LO1, LO2, PH, V3CD, and V4t), and the frontal eye fields (FEF).

V8 receives from V2, V3 and V4 and PIT and the FFC, and connects to ventromedial visual areas VMV1-VMV3 and VVC. Because these ventromedial areas connect with

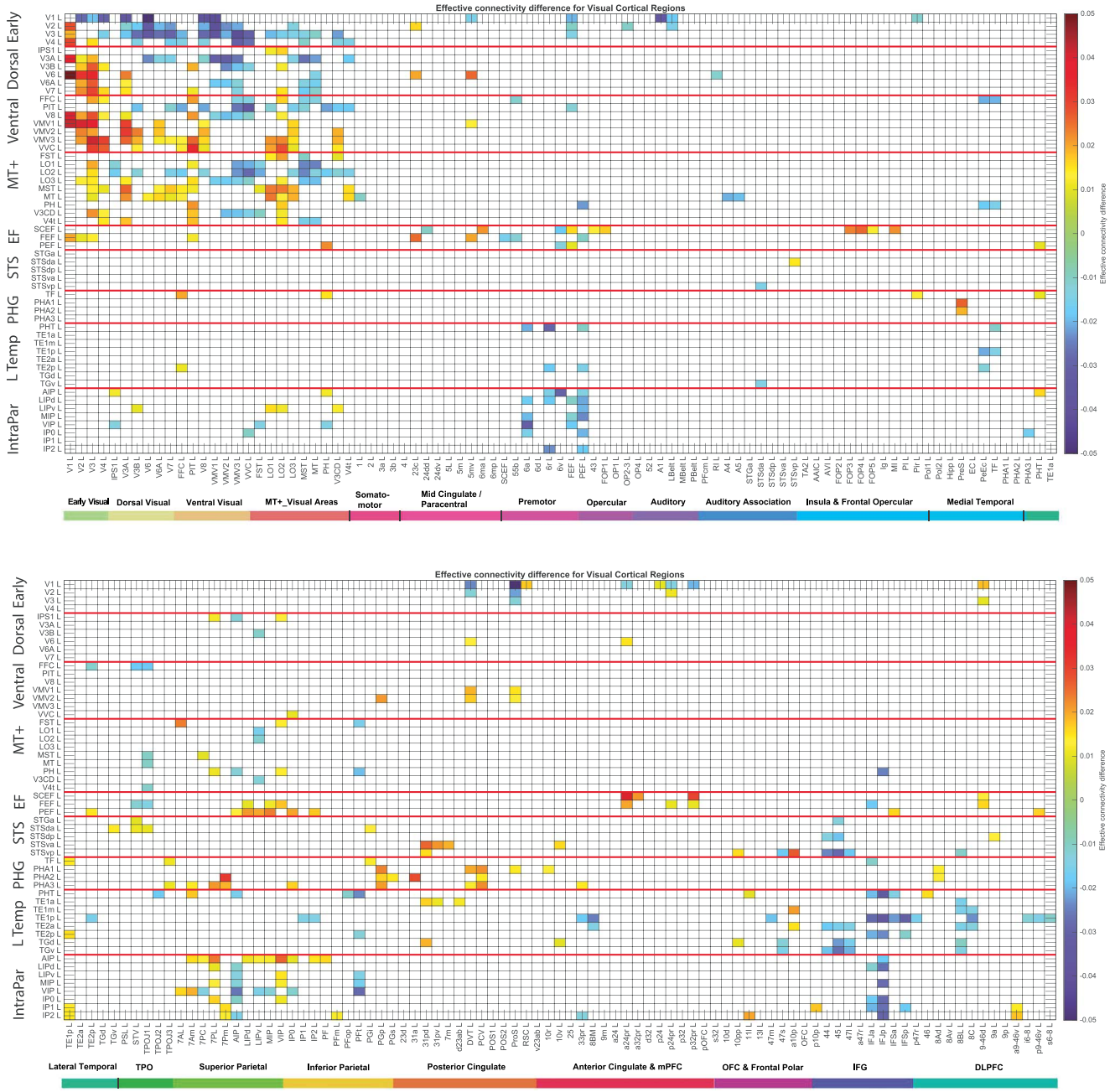

Fig. 3. Difference of the effective connectivity for visual cortical regions with other cortical regions. For a given link, if the effective connectivity difference is positive, the connectivity is stronger in the direction from column to row. For a given link, if the effective connectivity difference is negative, the connectivity is weaker in the direction from column to row. This is calculated from 171 participants in the HCP imaged at 7T. The threshold value for any effective connectivity difference to be shown is 0.01. The abbreviations for the brain regions are shown in Table S1, and the brain regions are shown in Figs.. 6–10 and S1. The effective connectivity difference for the first set of cortical regions is shown in the top panel; and for the second set of regions in the lower panel. Conventions as in Fig. 1.

parahippocampal gyrus TH (PHA1-PHA3) regions, they provide a route for ventral visual stream processing to reach the hippocampal system. In the Discussion, this ventromedial stream is shown to be involved in scene processing.

VMV1 receives from V1, V2, V3, V3A, V6A, and V8; and also from DVT and the prostriate region ProS (which two constitute the retrosplenial scene area RSC (Sulpizio et al. 2020; Rolls, Wirth, et al. 2022f)). It has bidirectional connectivity with V6. It also receives some connectivity from LO3, and 5mv. It has strong effective connectivity with VMV2 (0.085), and moderate (0.023) with VMV3.

VMV2 receives from V2, V3, V3A, V3B, V6, V6A, and V8; and also from DVT and ProS. It has bidirectional connectivity with V6. It also receives some connectivity from LO3, and V3CD; and from the parietal region PGp (which in turn is connected with superior parietal visual regions (Rolls, Deco, et al. 2022a)). VMV2 has strong effective connectivity with VMV1 andVMV3, and moderate with VVC. VMV2 has moderate effective connectiv

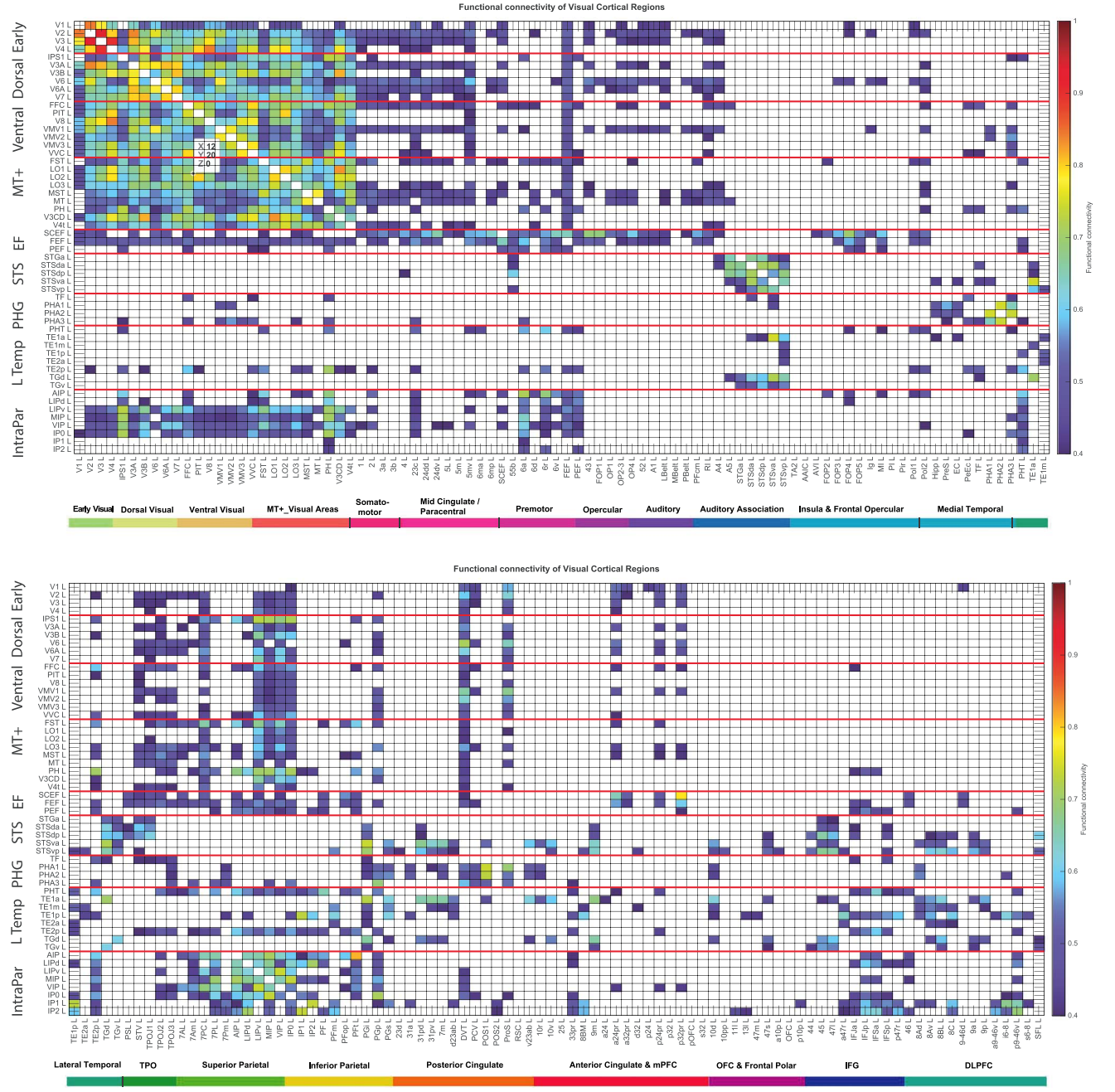

Fig. 4. Functional connectivity between visual cortical regions and 180 other cortical regions in the left hemisphere. Functional connectivities less than 0.4 are shown as blank. The upper figure shows the functional connectivity of the visual cortical regions with the first half of the cortical regions; the lower figure shows the functional connectivity with the second half of the cortical regions. Abbreviations: See Table S1. Conventions as in Fig. 1.

ity with parahippocampal PHA3, and some with PHA1 (Figs. 1–3).

VMV3 receives from V3, V4, V3B, V6, V6A, V7, and V8. It also receives some connectivity from MT+ Complex regions (LO1, LO2, LO3, and V3CD); and from the parietal region IP0. VMV3 has strong effective connectivity with VMV2 and VVC, and moderate with VMV1 (Figs. 1–3).

VVC receives from V2, V3, V4, V3A, V3B, PIT. It has moderate bidirectional connectivity with FFC and V8. It also receives some connectivity from MT+ Complex regions (LO1, LO2, LO3, PH, and V3CD; and from the parietal region PGp (which in turn is connected with superior parietal visual regions (Rolls, Deco, et al. 2022a)). VMV3 has strong effective connectivity with VMV3, and moderate with VMV2 (Figs. 1–3). VVC has outputs to hippocampal system PHA3, with some also to perirhinal cortex PeEc and TF.

Overall, the connectivity of these ventral stream visual division areas provides evidence for connectivity of early visual cortical areas (V2, V3, V4, etc.) to two cortical visual systems. One proceeds via FFC to inferior temporal visual cortex regions, which are involved in object and face perception, also provide "what" inputs to the hippocampal

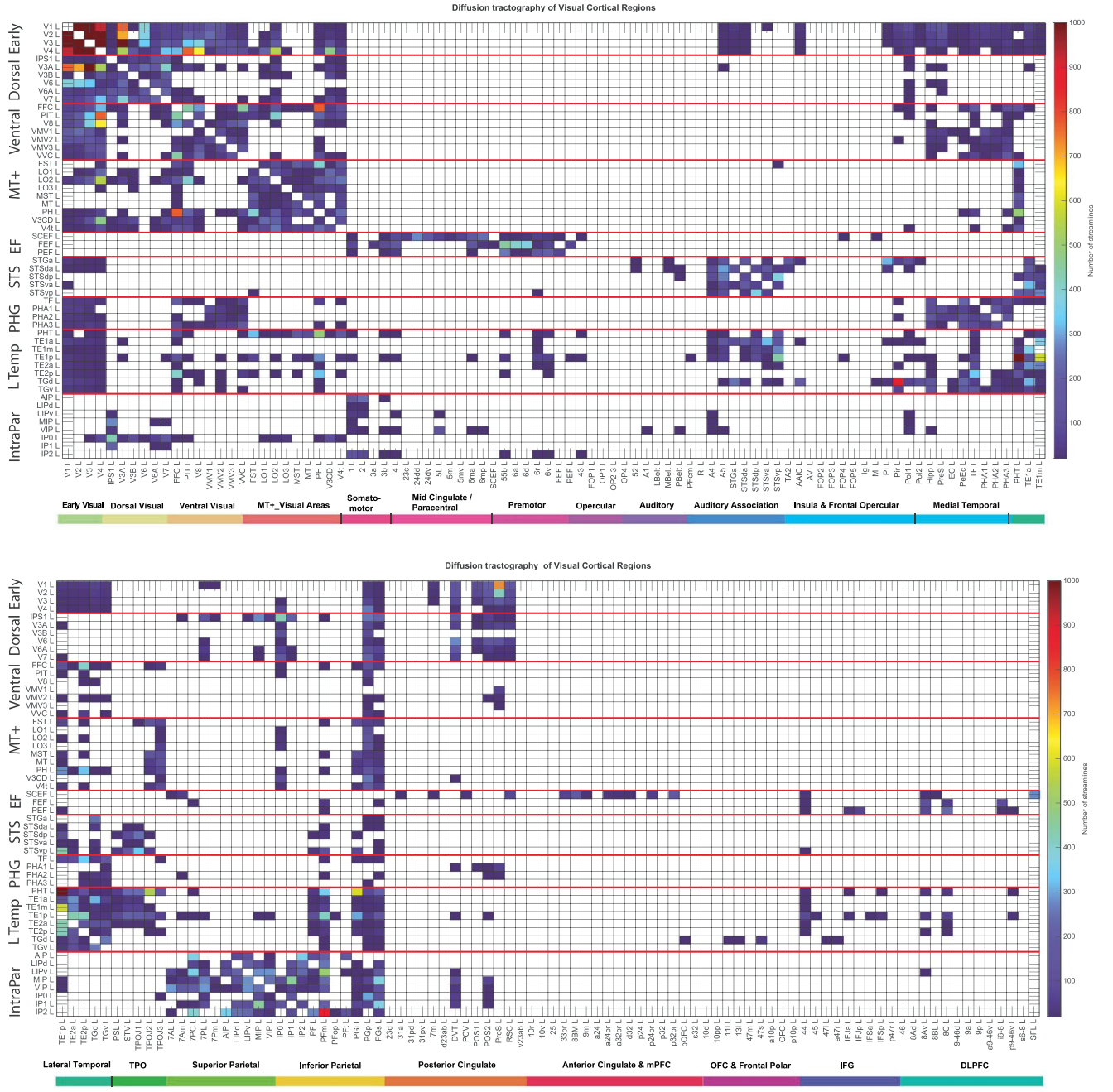

Fig. 5. Connections between the visual cortical regions and 180 other cortical regions in the left hemisphere as shown by diffusion tractography using the same layout as in Figs. 1 and 4. The number of streamlines shown was thresholded at 10 and values less than this are shown as blank. The color bar was threshold at 1000 streamlines (see text). Abbreviations: See Table S1. Conventions as in Fig. 1.

system via TF and perirhinal cortex, and also project to TPOJ regions implicated in language. The second proceeds via V8 and PIT to the ventromedial visual areas (VMV1-VMV3 and VVC) and thus to the hippocampal gyrus especially PHA regions in the scene part of the parahippocampal gyrus and thus provide "scene where" inputs to the hippocampal memory system. Both ventral visual stream branches are not only for static visual object and scene information, but also receive visual motion inputs from e.g. the MT+ complex regions. The evidence for these functional points is provided in the Discussion.

MT+ complex division: FST, lateral occipital areas 1–3 LO1-LO3, MST, MT, PH, V3CD and V4t.

FST (which stands in macaques for fundus of the superior temporal sulcus) receives from LO1 and LO2, and has reciprocal connectivity with IPS1, FFC, some other MT+ regions (LO3, MST, PH and V4t), some area 7 regions (7AL, 7PC); some intraparietal regions (AIP, LIPv, VIP); and inferior parietal PFt.

LO1 receives from V3, and has generally bidirectional connectivity with V4, IPS1, V3A, V3B, V7, FFC, PIT, V8, LO2, LO3, V3CD, and V4t. It has connectivity directed to FST, MST, MT, PH, and LIPv. This is more than a visual motion

region, in that it has connectivity with ventral stream FFC and PIT.

LO2 receives from V3, and has generally bidirectional connectivity with V4, V3B, V7, FFC, PIT, V8, LO1, LO3, V3CD, and V4t. It has connectivity directed to VMV3, VVC, FST, MST, MT, PH, and LIPv. This is more than a visual motion region, in that it has connectivity with ventral stream FFC and PIT.

LO3 receives from V3, and has generally bidirectional connectivity with V3A, V3B, V6, V6A, V7, FFC, LO1, LO2, V3CD, and V4t, FST. It has connectivity directed to VMV1, VMV2, VMV3, VVC, FST, MST, MT. It also has some connectivity with TPOJ1 and TPOJ2, VIP, and PGp. LO3 is of interest in providing inputs to all the ventromedial visual regions (VMV1-VMV3 and VVC), which in turn connect to the scene parahippocampal system (Rolls, Deco, et al. 2022d).

MST receives from V3, V4, V3A, V3B, V6A, V7, FFC, PIT, LO1, and LO2 and has generally bidirectional connectivity with FST, LO3, MT, V4t, TPOJ2, TPOJ1, and 7PC.

MT receives from V3, V3A, V6, V6A, V7, FST, LO1, LO2, and 7PC and has generally bidirectional connectivity with FFC, MST, V4t, STV. Interestingly, it projects to A4 and A5, and has bidirectional connectivity with multimodal language-related TPOJ3, TPOJ1, TPOJ3.

PH receives from PIT and LO2, and has generally bidirectional connectivity with IPS1, FFC, VVC, FST, V3CD, AIP, LIPd, LIPv, MIP, VIP, and IP0. It projects to the premotor eye field PEF, to the hippocampal system (perirhinal cortex PeEc and TF), to lateral temporal regions PHT and TE2p, to PFt, and to the inferior frontal region IFJp. It is thus not a typical MT+ Complex region, for it combines connectivity with visual motion areas with connectivity with ventral stream object areas such as PHT and TE2. PH is a large region (Table S1), and perhaps will be subdivided in future.

V3CD receives from V3 and V3A, and has generally bidirectional connectivity with V4, IPS1, V3B, V7, FFC, PIT, V8, VMV3, VVC, LO1, LO2, LO3, PH, V4t, LIPv VIP, and IP0. It connects to VMV2. It thus combines ventral stream and dorsal motion information, and has connectivity with the VMV scene region. V3CD, V3B, and IP0 form the occipital place area OPA (Sulpizio et al. 2020).

V4t receives from V3, V4, and V3A, and has generally bidirectional connectivity with V6A, V7, FFC, PIT, FST, LO1, LO2, LO3, MST and MT, and 7PC. It has some connectivity directed to somatosensory regions (1 and 5m), and to TPOJ1. It therefore has connectivity with visual motion regions, but also some connectivity with object/processing ventral stream regions FFC and PIT.

Eye field regions: supplementary and cingulate eye field SCEF, frontal eye fields FEF, premotor eye fields PEF.

The SCEF receives from the supracallosal anterior cingulate cortex (a24pr, a32pr, p32pr) (which have somatosensory connectivity (Rolls, Deco, et al. 2022e)) and from other somatosensory/premotor areas (mid-cingulate 24dv; 5mv, 6ma, 6mp, 55b, 6r, 6v, 43, FOP1, FOP3, FOP4, FOP5, and mid-insula MI). There is also bidirectional connectivity with FEF and PEF. There is a weak input from V1. This appears to be more a somatosensory than eye movement region, though it does have connectivity with FEF and PEF, which are more typical eye field regions.

The FEF receives from V1, V2, V3, FFC, PIT, LIPd, LIPv, MIP, and VIP. It also does have somatosensory/premotor connectivity (from mid-cingulate 23c, from 5mv, with 6ma, 55b, 6a, 6r, FOP4, FOP5, a24pr, p24pr, p32pr). It also has some connectivity directed more towards than from some multimodal/language-related regions including the PeriSylvian Language region PSL, STV, TPOJ1, and TPOJ2 (Rolls, Deco, et al. 2022c). There is also connectivity with PEF and SCEF.

The PEF receives from some visual regions (IPS1, PH, PHT, TE2p, AIP, LIPd, LIPv, MIP, IP0, IP2). It also does have somatosensory/premotor connectivity (55b, 6a, 6r, 6v). It has connectivity with SCEF and FEF, and also with a set of short-term-memory-related inferior frontal areas (IFJa, IFJP, IFSa, IFSp, and receives from the dorsolateral prefrontal cortex p9-46v.

Superior Temporal Sulcus cortical regions: STGa, STS dorsal anterior STSda, STS dorsal posterior STSdp, STS ventral anterior STSva, STS ventral posterior STSvp.

STGa in the superior temporal gyrus at the temporal pole has strong connectivity with STSda, STSdp (which themselves have some connectivity with visual motion regions) and weaker with STSva. STGa also has effective connectivity with auditory regions A5, A4, and TA2. It also has connectivity with language-related regions in the temporal pole (TGd and TGv) and in temporo-parieto-occipital regions PSL, STV, and TPOJ1; with the superior frontal language area SFL; and with 55b. STGa connects to part of Broca's area, area 45 (Figs. 1–3). STGa is proposed to be part of a superior (i.e. dorsal) STS cortex semantic system including STSda and STSdp, which in involved in multimodal auditory and corresponding visual motion information (Rolls, Deco, et al. 2022c).

STSda in the dorsal anterior part of the superior temporal sulcus receives from parietal cortex visual region PGi, which is a multimodal visual region that combines visual object with visual motion inputs (Rolls, Deco, et al. 2022a). STSda has strong connectivity with STGa, STSdp, STSva and more weakly with STSvp. STSda also has effective connectivity with auditory region A5. It also has connectivity with language-related regions in the temporal pole (TGd and TGv) and temporo-parieto-occipital regions STV and TPOJ1. STSda has connectivity with parahippocampal TF, which provides inputs to the hippocampus (Rolls, Deco, et al. 2022d), and with a memory-related part of the posterior cingulate cortex (31pd) (Rolls, Wirth, et al. 2022f). STSda connects to part of Broca's area, area 45 (Figs. 1–3).

STSdp in the dorsal posterior part of the superior temporal sulcus receives from parietal cortex visual region PGi. STSdp has strong connectivity with STGa, STSda, STSvp, and more weakly with STSva. STSdp also

has effective connectivity with auditory region A5. It also has connectivity with language-related regions in the temporal pole (TGd and TGv), in temporo-parieto-occipital areas PSL, STV, and TPOJ1; with SFL; and with a left lateral orbitofrontal cortex region 47l, which is also part of the language network (Rolls, Deco, et al. 2022c). STSdp connects to part of Broca's area, regions 45 and 44 (Figs. 1–3). This connectivity provides evidence that STSdp is part of a superior (dorsal) STS semantic network with visual and auditory components (Rolls, Deco, et al. 2022c).

STSva in the ventral anterior part of the superior temporal sulcus receives strong visual effective connectivity from object-related inferior temporal visual cortex TE1a; and it also receives strongly from inferior parietal visual region PGi. It has strong effective connectivity with STSda and TGd, and moderate with STGa, STSdp, STSvp. STSva has moderate effective connectivity with the hippocampal system via parahippocampal TF and the posterior cingulate cortex memory-related regions 31pd, 31pv, v23ab, and the related medial parietal 7m (Rolls, Wirth, et al. 2022f). It also has effective connectivity with the reward-related ventromedial prefrontal cortex (vmPFC) 10v and pregenual anterior cingulate cortex 9m.

STSvp in the ventral posterior part of the superior temporal sulcus receives strong visual effective connectivity from object-related inferior temporal visual cortex TE1a, TE1m, TE2a; and it also receives strongly from inferior parietal visual regions PGi and PFm (Rolls, Deco, et al. 2022a). It has strong effective connectivity with STSdp and STSva, and moderate with STSda, STSvp; and TGv and TGd. STSvp has some effective connectivity with the hippocampal system via the posterior cingulate cortex memory-related regions 31pd and 31pv (Rolls, Wirth, et al. 2022f). It also has effective connectivity with the reward-related ventromedial prefrontal cortex 10v and pregenual anterior cingulate cortex 9m. It also has effective connectivity to language-related areas 45, 44, 47s, and 47r on the left and with the Superior Frontal Language region SFL, and premotor 55b (Rolls, Deco, et al. 2022c). STSvp also has effective connectivity with dorsolateral prefrontal cortex short-term memory-related regions 8Av, 8BL, 8C, and 9a. It is therefore proposed that STSvp is part of a ventral STS cortex semantic system with visual input from the inferior temporal visual cortex and parietal visual areas PGi and PFm, and links these into a semantic system with outputs to Broca's area, which is implicated in syntax (Friederici et al. 2017; Rolls, Deco, et al. 2022c).

Parahippocampal gyrus regions: TF; and parahippocampal areas 1–3 PHA1-PHA3 (which correspond to macaque TH).

TF is a relatively anterior and lateral part of the parahippocampal gyrus (Figs. 6–10 and Fig. S1). TF receives effective connectivity from ventral visual stream regions FFC, PH, PHT, TE1p, TE2b, and some also from parietal visual region PGi. It also has connectivity with STSda, STSva, and TGd. It receives olfactory effective connectivity from the pyriform cortex (Pir), and has connectivity with orbitofrontal cortex 47m, which is a punishment/reward emotion-related region (Rolls, Deco, et al. 2022e). It also has connectivity with some language-related regions (STV, TPOJ1, TPOJ2, and TPOJ3) (Rolls, Deco, et al. 2022c). TF has strong effective connectivity with the perirhinal cortex (PeEc), which is a ventral "what"/emotion gateway to the hippocampal memory system (Rolls, Deco, et al. 2022d). It is thus proposed that TF is a part of the parahippocampal gyrus that provides a route for lateral ventral "what" information about objects and faces, and reward/punishment information, to enter the hippocampal memory system (Rolls, Deco, et al. 2022d). It is important to note that this part of the parahippocampal gyrus is connected to "what" systems, for in macaques the emphasis has been in the past that the parahippocampal gyrus is a parietal "where" route to the hippocampus at a similar level to perirhinal cortex for "what" information (Van Hoesen 1982).

PHA1-PHA3 in the HCP-MMP atlas are relatively posterior and medial parts of the parahippocampal gyrus that correspond to macaque TH.

PHA1 has connectivity with visual areas parieto-occipital sulcus POS1, prostriate ProS, and the dorsal visual transitional region (DVT) (which latter two are the retrosplenial place area (Sulpizio et al. 2020)), and from PGp in the inferior parietal cortex, which has connectivity with parietal visual motion regions (Rolls, Deco, et al. 2022a). PHA1 has connectivity with the hippocampal system (Hipp, presubiculum PreS, entorhinal cortex EC) and with PHA2 and PHA3. It also has weak connectivity with VMV2. It also has some connectivity with the posterior cingulate cortex (PCV) and from the ventromedial prefrontal cortex 10r.

PHA2 has connectivity with visual areas parieto-occipital sulcus POS1 and prostriate ProS, and from visual regions PGp and PGs in the inferior parietal cortex, which have connectivity with parietal visual motion regions (Rolls, Deco, et al. 2022a), and from 7Pm. PHA2 has connectivity with the hippocampal system (presubiculum PreS, entorhinal cortex EC); and with PHA1 and PHA3.

PHA3 has connectivity with ventromedial visual regions VMV2 and VVC; and prostriate ProS, and from visual region PGp in the inferior parietal cortex; and from 7Am, 7PL, 7Pm and IP0. PHA2 has connectivity with the hippocampal system (perirhinal and TF) and with PHA1 and PHA2.

PHA1–3 thus provide a route for information from ventromedial visual regions such as VMV2 and VVC, and for parietal visual motion regions including from inferior parietal (PGp, PGs), intraparietal, and area 7 to reach the hippocampal memory system but also potentially to interact with each other in PHA1-PHA3.

Lateral temporal division: PHT, TE1 anterior TE1a, TE1 middle TE1m, TE1 posterior TE1p, TE2 anterior TE2a, TE2

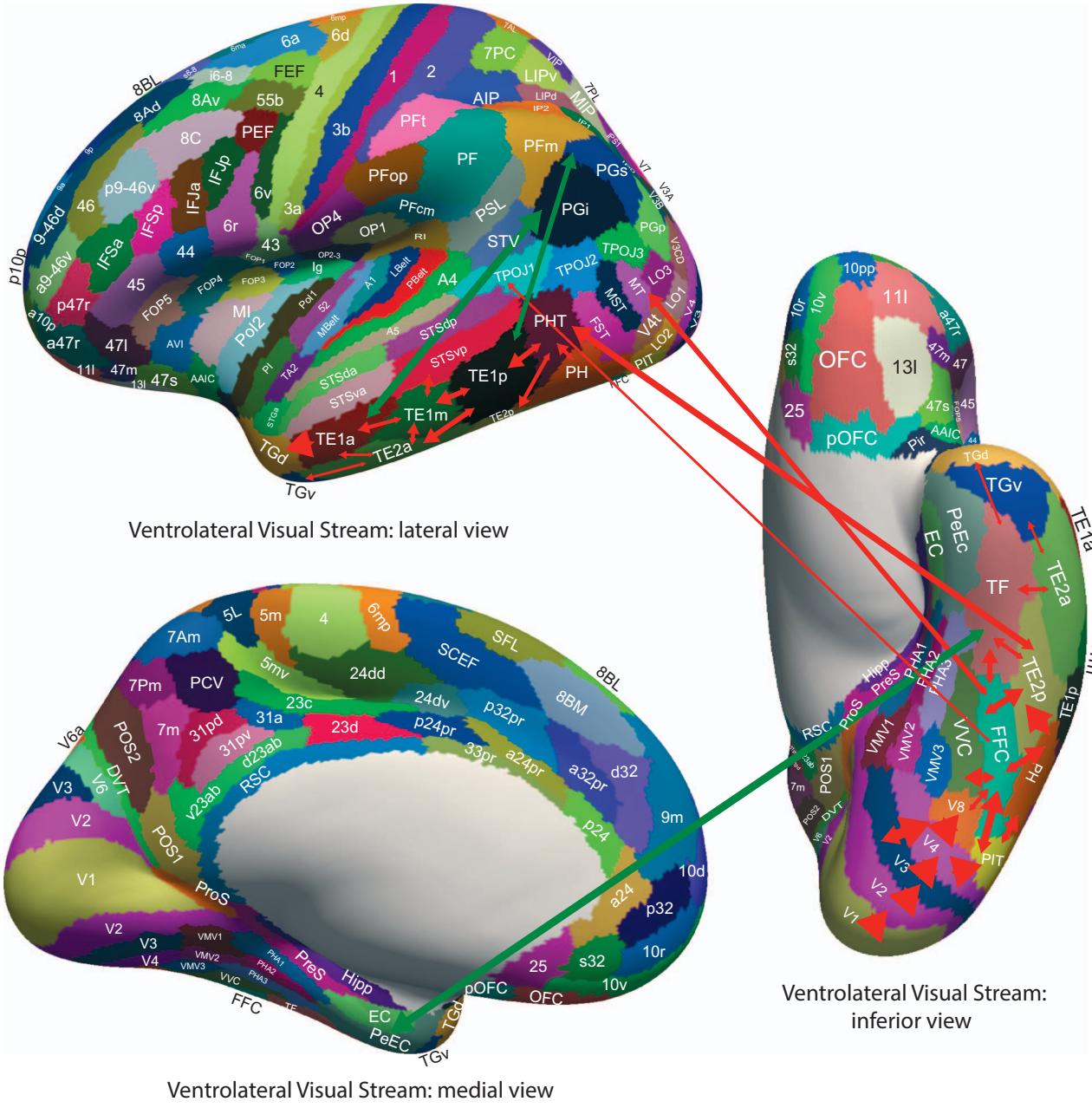

Fig. 6. Effective connectivity of the Ventrolateral Visual Cortical Stream, which reaches inferior temporal cortex TE regions in which objects and faces are represented: Schematic overview. A green arrow shows how the Ventrolateral Visual Stream provides "what" input to the hippocampal memory system via parahippocampal gyrus TF to perirhinal PeEc connectivity from FFC, PH, TE1p, TE2a and TE2p. The Ventrolateral Visual Stream also provides input to the semantic language system via TGd. The Ventrolateral Visual Stream also has connectivity to the inferior parietal visual area PFm, PGs and PGi as indicated by 2 green arrows. The widths of the lines and the size of the arrowheads indicate the magnitude and direction of the effective connectivity.

posterior TE2p, temporal pole TG dorsal TGd, temporal pole ventral TGv.

PHT has effective connectivity with visual regions PH, TE1p, TE2p, 7Am, 7PL, AIP, LIPd, MIP, IP0, IP2, and PGp. PHT also has connectivity with parietal somatosensory areas PF, PFop, and PFt and supracallosal anterior cingulate 33pr and p24pr; and connectivity to the PEF and premotor regions 6a, 6r and in the midcingulate cortex 23c. PHT also receives some input from the reward-related medial orbitofrontal cortex (11l and 13l) and has some connectivity with the lateral orbitofrontal cortex 47r (Rolls, Deco, et al. 2022e). PHT also has connectivity with inferior prefrontal and dorsolateral prefrontal short-term memory-related regions.

A feature of the TE1 and TE2 inferior temporal visual object and face areas in the lateral ventral visual stream is their effective connectivity with inferior parietal visual regions such as PGi. The TE1 regions are lateral to the TE2 regions (Figs. 6–10 and Fig. S1).

TE1a (anterior) has effective connectivity with inferior temporal visual TE1m, TE2a; with inferior (ventral) STS regions STSva and STSvp, and TGd; interestingly with inferior parietal PGi and PGs; and with medial parietal 7m, which is part of the precuneus. TE1a also has

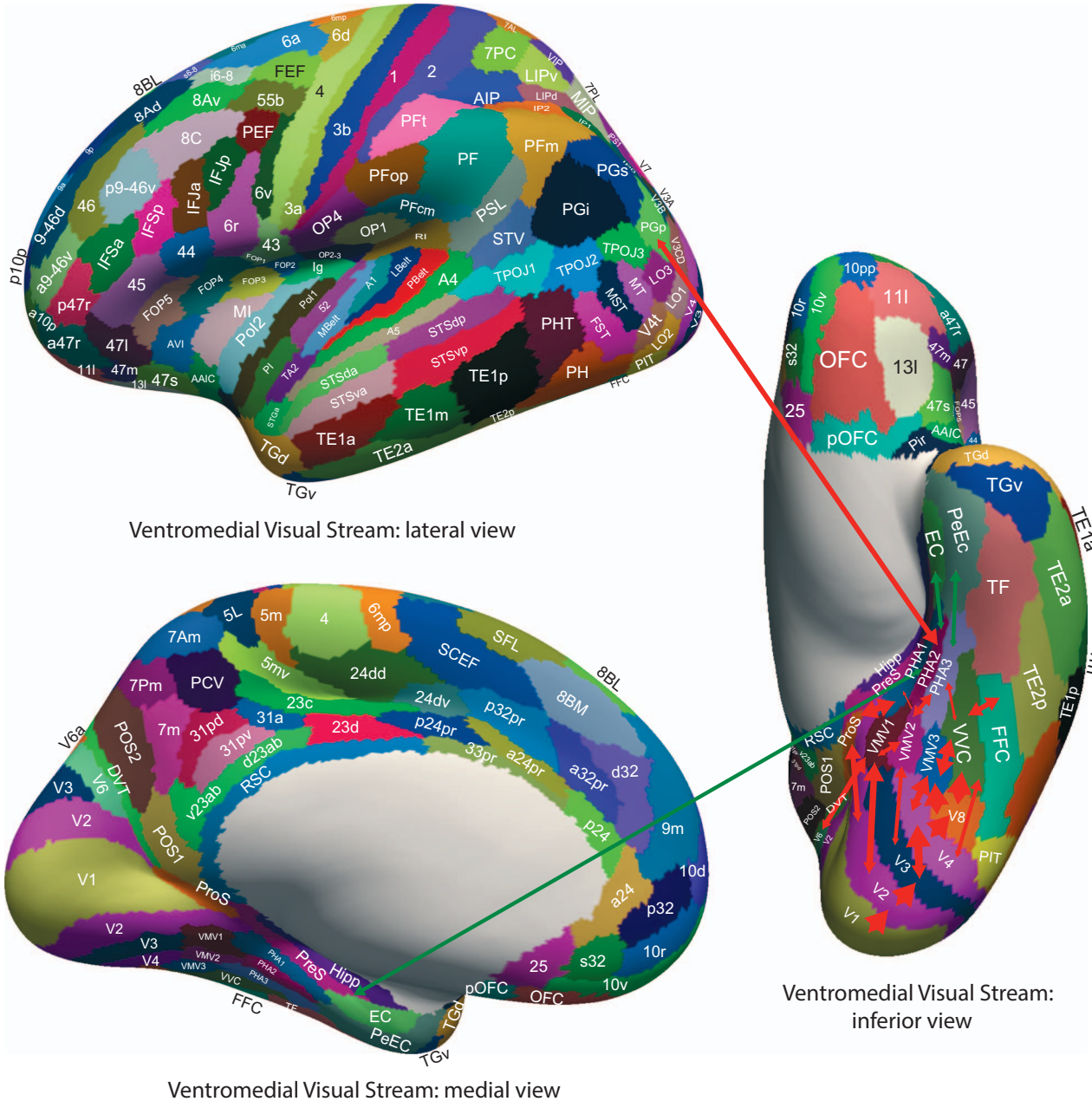

Fig. 7. Effective connectivity of the Ventromedial Visual Cortical Stream, which reaches the parahippocampal gyrus PHA1—PHA3 regions via ventromedial (VMV) and ventral visual complex (VVC) and ProStriate regions: Schematic overview. Visual scenes are represented in the anterior parts of VMV and the posterior parts of PHA1—PHA3 in what is the Parahippocampal scene area PSA (sometimes called the Parahippocampal place area, PPA). The green arrows show how the Ventromedial Visual Stream provides "where" input about locations in scenes to the hippocampal memory system from the parahippocampal gyrus PHA1- PHA3 region (which corresponds to TH in macaques). The connectivity from PGp to PHA regions is suggested in the text to be involved in idiothetic update of locations in scenes. The widths of the lines and the size of the arrowheads indicate the magnitude and direction of the effective connectivity.

connectivity with reward-related vmPFC 10v and 10d and pregenual anterior cingulate cortex (ACC) 9m (Rolls, Deco, et al. 2022e); with memory-related parts of the posterior cingulate cortex 31pd, 31pv, d23ab, and v23ab (Rolls, Wirth, et al. 2022f); and with the dorsolateral prefrontal cortex.

TE1m (middle) has effective connectivity with inferior temporal visual areas TE1a, TE1p, and TE2a and with inferior STS region STSvp, and also with inferior posterior parietal cortex regions PGi, PGs, and PFm, which are visual (Rolls, Deco, et al. 2022a). TE1 also has connectivity with reward/punishment-related vmPFC 10d and orbitofrontal cortex OFC and a47r. TE1m also has connectivity with posterior cingulate cortex d23ab, and with dorsolateral prefrontal regions 8 (Figs. 1–3).

TE1p (posterior) has effective connectivity with inferior temporal visual areas TE1a, TE1p, and TE2a and with inferior STS region STSvp, and also with inferior posterior parietal cortex regions PGi, PGs and PFm, which are visual (Rolls, Deco, et al. 2022a). TE1 also has connectivity with reward/punishment-related vmPFC 10d and orbitofrontal cortex OFC and a47r.

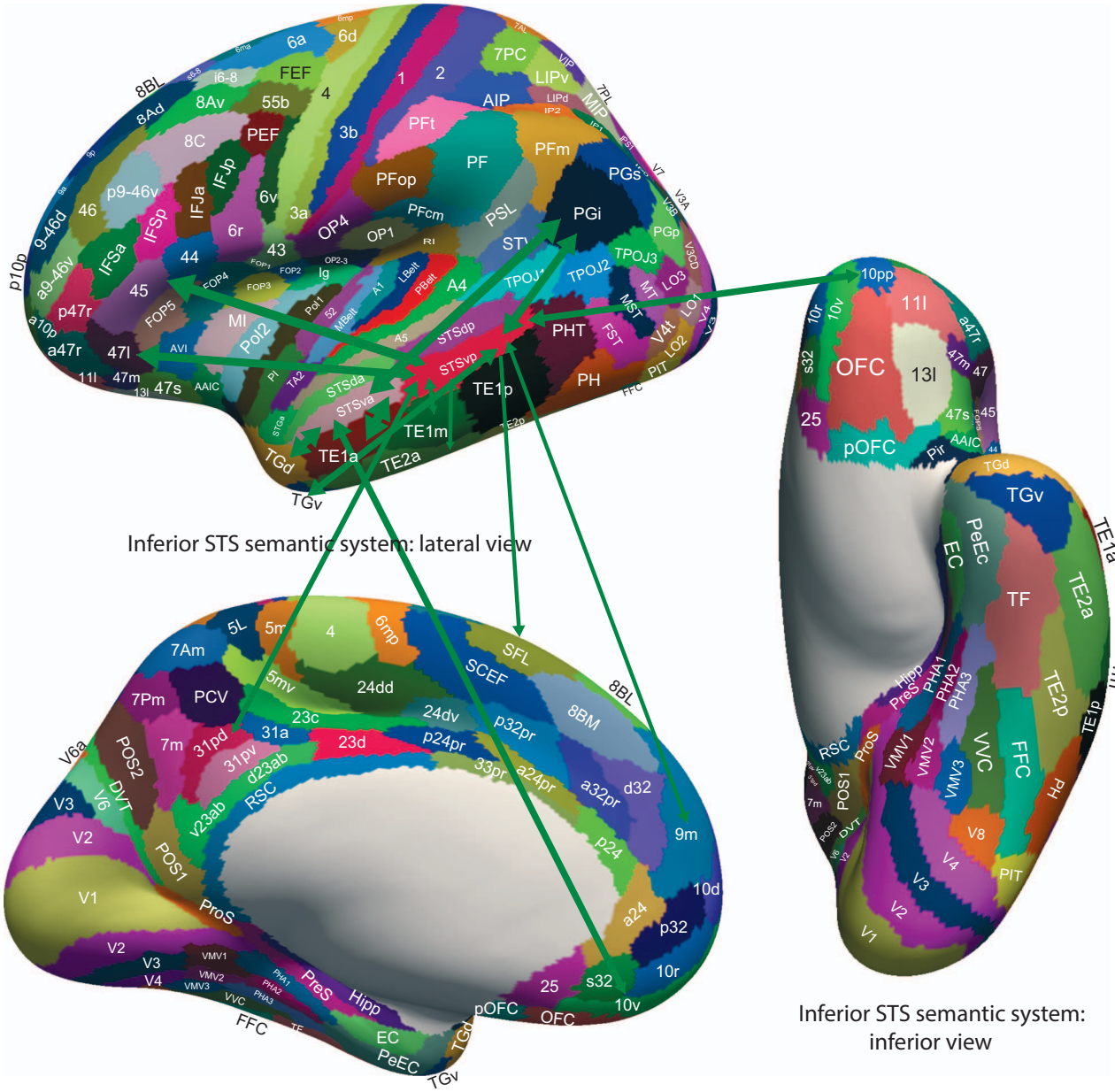

Fig. 8. Inferior STS cortex semantic system in STSva and STSvp: schematic overview. An output of the ventrolateral visual system for object and face information is to the cortex in the inferior parts of the Superior Temporal Sulcus, STSva and STSvp. The visual inputs to these inferior STS cortex regions are shown with green arrows, and come from TE1a, TE1m, TE2a, TGd, TGv, and PGi. Other connectivities are with the memory-related parts of the posterior cingulate cortex (31pd and 31pv); and from the vmPFC (10v and 10r) (see Fig. 1). STSva and STSvp have connectivity directed towards Broca's area 44 and 45, and related areas (47s), and to the superior frontal language region (SFL) (Rolls, Deco, et al. 2022c).

TE1m also has connectivity with posterior cingulate cortex d23ab, and with dorsolateral prefrontal regions 8 (Figs. 1–3).

TE2a has effective connectivity with TE1m, TE1p, and TE1a; and with STSvp, and temporal pole TGv and TGp. TE2a also has effective connectivity with PFm and PGi. TE2a also receives from the frontal pole a10p, has connectivity with the orbitofrontal cortex 47l, a47r and p47r and dorsolateral prefrontal area 8 regions. TE2a connects to the hippocampal system via TF. Interestingly, TE2a also has connectivity directed to Broca's area 44 and 45.

TE2p has effective connectivity with more posterior visual cortex regions including PH, PHT, FFC, and FST. It also has connectivity with intraparietal regions (AIP, LIPd, MIP and IP0). It also has connectivity with TPOJ2 and TPOJ3; with the hippocampal memory system (perirhinal PeEc, and TF); with the supracallosal anterior cingulate 33pr; to the PEF and 6r; and with inferior prefrontal cortex regions (IFJa, IFJp, IFSa, IFSp). One point of interest here is that TE2p has only weak effective connectivity to other TE regions, with the connectivity from TE2p to TE1p only 0.0004, and more connectivity in the reverse

direction (0.016) and a reasonable number of streamlines (419) as shown in Fig. 5.

TGd in the temporal pole has strong effective connectivity with TE1a, TGv, and the STS regions (STGa, STSda, STSdp, STSva, STSvp), and PGi (Figs. 1–3). It has strong connectivity with reward-related vmPFC 10v, and pregenual anterior cingulate 9m. It has connectivity with the hippocampal memory system via TF and via posterior cingulate 31pd (Rolls, Wirth, et al. 2022f), and with the dorsolateral prefrontal short-term memory related regions 8BL, 9a, and 9p. It has connectivity directed to Broca's region 45 and its closely connected regions in the left hemisphere 47s and 47l (Rolls, Deco, et al. 2022c).

TGv has strong effective connectivity with TGd, and the STS regions (STGa, STSda, STSdp, STSvp), and moderate with STSva and TE2a (Figs. 1–3). It has connectivity with the dorsolateral prefrontal short-term memory related regions 8BL and 9a. It has connectivity directed to Broca's region 44, and has connectivity with other language-related areas including 45, 47s, and 47l, the PeriSylvian Language region (PSL) and the Superior Frontal Language region SFL and 55b in the premotor cortex (Rolls, Deco, et al. 2022c).

Intraparietal sulcus posterior parietal cortex: AIP, LIPd, LIPv, MIP, VIP (with IP0, IP1 and IP2).

As shown in Fig. 1, these regions have strong effective connectivity from early visual cortical areas including dorsal visual intraparietal sulcus area 1 (IPS1), V3B, V6A, and V7; ventral visual FFC, and posterior inferotemporal PIT and PHT; from several MT+ complex visual regions including FST, LO1, LO3, PH, and V3CD; from premotor regions especially 6a, 6r and the premotor eye field PEF; strongly from visual anterior inferotemporal TE1p and TE2p; from area 7 regions; from inferior parietal regions including PGp; from the orbitofrontal cortex (medial regions, 11 and OFC); frontal pole p10p; from the inferior frontal gyrus; and extensively with the dorsolateral prefrontal cortex, especially 8C, a9-46v, i6-8, and p9-46v. Many of these connectivities are reciprocated (Fig. 2), but the effective connectivities are stronger to the intraparietal areas from early visual cortical areas, TE1p (to IP1 and IP2), area 7 regions, and the medial orbitofrontal cortex (Fig. 3), indicating that these are mainly input areas to the intraparietal regions. Conversely, the effective connectivities are stronger from the intraparietal areas to premotor areas (6a, 6r, and PEF); and to the inferior frontal gyrus regions (IFJ); and to the parahippocampal gyrus TH (Figs. 2 and 3), providing evidence that these are output pathways from the intraparietal cortex.

The functional connectivity is consistent (Fig. 4), but indicates more interactions with early visual cortical areas including the ventromedial visual areas (VMV) implicated in scene perception (Sulpizio et al. 2020); with somatosensory/premotor areas; with the hippocampal system; with TE1p and TE2p; with posterior cingulate/early visual DVT; and with supragenual anterior cingulate 33pr and p24pr (Rolls, Deco, et al. 2022e).

The diffusion tractography (Fig. 5) is also consistent, and emphasizes connections with somatosensory-premotor cortex; shows some connections with auditory cortex; and with the posterior cingulate cortex especially the dorsal transitional visual area DVT implicated in scene perception (Sulpizio et al. 2020; Rolls, Wirth, et al. 2022f).

Effective connectivities of the 55 visual cortical regions with contralateral cortical regions

The effective connectivities of the 55 visual cortical regions from contralateral cortical areas are shown in Fig. S2, and to contralateral cortical regions in Fig. S3.

A feature of the effective connectivities is that they are strongest to the corresponding brain region contralaterally. This is shown for example by the diagonal line of high effective connectivities in Figs. S2 and S3 from V1 to V4t, from TF to PHA3, in the lateral temporal regions, and in the intraparietal regions where the order of brain areas is the same for the rows and columns so that the diagonal lines of high connectivity stand out. This attests to the power of the effective connectivity algorithm, for it detects corresponding particular brain regions in the contralateral hemisphere. Also, this is an interesting principle of brain connectivity, which implies that the contralateral connectivities provide especially for comparison and support between regions performing similar processing in the other hemisphere, rather than providing for hierarchical computations between the 2 hemispheres.

The contralateral effective connectivities are in general weaker than those ipsilaterally. The ratio across the matrices shown in Fig. 1 and Fig. S2 was that the contralateral effective connectivities were 66% of the ipsilateral effective connectivities.

Differences of effective connectivities of the right vs left hemisphere for the 55 visual cortical regions

Most of the analyses presented so far have been for the left hemisphere, or of the left hemisphere with the right hemisphere. For completeness, the differences of effective connectivity for the right minus the left hemisphere for the 55 visual cortical regions are shown in Figs. S6 and S7. One implication of what is shown in Figs. S6 and S7 is that the connectivities of the dorsal, ventral, MT+ and intraparietal divisions are stronger in the right than the left hemisphere. This is consistent with concepts that visual processing is somewhat more a feature of the right than the left hemisphere. For the STS regions, the reverse is the case, and the connectivities in the left hemisphere are generally stronger, consistent with their connectivity with language regions of the cortex in the left hemisphere. The parahippocampal connectivities with the hippocampal system, and with VMV areas implicated in scene representations (Sulpizio et al. 2020; Rolls, Deco, et al. 2022d), are stronger in the right hemisphere.

Functional connectivity and diffusion tractography

The functional connectivity is shown in Fig. 4 and the diffusion tractography in Fig. 5 for comparison with the effective connectivity. Functional connectivity and diffusion tractography have been used in many previous investigations of the human connectome (Catani and Thiebaut de Schotten 2008; Glasser, Coalson, et al. 2016a; Maier-Hein et al. 2017), and therefore the comparison with effective connectivity is of interest.

The functional connectivities (Fig. 4), which represent a linear measure of connectivity (calculated with the Pearson correlation) range from close to 1.0 to −0.33 and with a threshold of 0.4 reveal somewhat more links than the effective connectivity, partly perhaps because they can reflect common input to two regions rather than causal connectivity between regions, and partly because the threshold has been set to reveal effects known in the literature but not reflected in the effective connectivity. The functional connectivities are useful as a check on the effective connectivities, but of course do not measure causal effects.

The diffusion tractography (Fig. 5) again provides no evidence on the direction or causality of connections, and is useful as it can provide some evidence on what in the effective connectivity may reflect a direct connection, and what does not. However, limitations of the diffusion tractography are that it cannot follow streamlines within the gray matter so the exact site of termination is not perfectly provided; and the tractography does not follow long connections well with for example almost none of the contralateral connectivity shown with tractography that is revealed by the effective connectivity in Figs. S2 and S3; and may thus overemphasize connections between close cortical regions. Nevertheless, the diffusion tractography is a useful complement to the effective connectivity, especially where it provides evidence where an effective connectivity link may be mediated by a direct connection. On the other hand, the effective connectivity and functional connectivity are useful complements to the tractography by helping to exclude false positives in the tract-following in the tractography, as had been examined for the human hippocampal connectome (Huang et al. 2021; Ma et al. 2022; Rolls, Deco, et al. 2022d).

Correlations between the connectivities of different cortical regions

Figure S4 emphasizes the similarity of the effective connectivities of the STS cortical regions with the connectivity of the temporal pole regions TGd and TGv. It also shows that regions IPS1, PH, and PHT have some similarities in their effective connectivity with the intraparietal areas (apart from IP1 and IP2, which have different connectivity to the other intraparietal regions). Figure S4 also emphasizes that parahippocampal PHA1-PHA3, which are part of the Ventromedial Visual Stream have similar connectivity to each other, and different connectivity to parahippocampal TF, which is part of the Ventrolateral Visual Stream (Rolls, Deco, et al. 2022d). Figure S4 also shows that the connectivities of the different inferior temporal cortical regions in the lateral temporal division are rather different from each other, indicating that these different regions are likely to make different information processing contributions. A comparison of Fig. S4 with Fig. S5, which shows the correlations between the functional connectivities of the 55 visual cortical regions, indicates that the effective connectivity is much more selective than functional connectivity in revealing the different connectivities of different cortical regions.

Discussion

The effective connectivities complemented by functional connectivity and diffusion tractography described here lead to the following proposed concepts and framework for the organization of the human visual system. The strengths of the effective connectivities are used as a guide; but also is the point made earlier that effective connectivity in the backward direction in a cortical hierarchical system does not reflect the transfer of the properties represented at a higher level but instead the capability for top–down attention and for memory recall; and so is evidence from neuronal recordings in comparable regions in macaques and activations in humans. This is the first large-scale investigation across all 360 cortical regions in the HCP-MMP atlas of the effective connectivity of the 55 visual cortical regions, with complementary evidence from functional connectivity and diffusion tractography analyses with the same 171 HCP participants. In the following, the results are discussed in terms of five cortical visual streams, but the emphasis is that there are multiple streams, not that there are exactly five. The five streams described here are selected partly on the basis of the effective connectivity described here, and partly on the known functions of the different regions towards which each stream has effective connectivity, as set out when each stream is considered below. The primary data are, however, in Figs. 1–5 and Figs. S2–S7, with Fig. S4 showing the correlations between the connectivities of each of the 55 visual cortex regions.

A Ventrolateral Visual Cortical Stream to the inferior temporal visual cortex for object and face representations

The Ventrolateral Visual Cortical Stream is characterized by effective connectivities that lead towards the inferior temporal visual cortex. After a progression from V1 > V2 > V3 > V4 (where > indicates the general progression but does not exclude some connectivity that is more than between strictly adjacent levels in the hierarchy), V4 (and to some extent V3) have effective connectivity to ventral division regions such as PIT and V8. PIT, and to some extent V8, then have connectivity to FFC (Figs. 1–3). FFC in turn has connectivity to TE2p and to PH (and PH

also connects to TE2p). PH and TE2p project to PHT, which in turn projects to TE1p, TE2a (and TPOJ2 and TPOJ3). We, therefore, have a route through the ventrolateral visual stream as shown schematically in Fig. 6. This stream provides "what" visual outputs to the orbitofrontal cortex/vmPFC reward/punishment emotion-related system (Rolls, Deco, et al. 2022e); to the hippocampal memory system (Rolls, Deco, et al. 2022d); to the language system (Rolls, Deco, et al. 2022c); and to the prefrontal cortex for short-term memory and planning.

Key discoveries about this Ventrolateral Visual Stream leading to the anterior inferior temporal visual cortex (IT) are that IT neurons code for objects and not their reward value (Rolls et al. 1977); that some neurons code for faces (Perrett et al. 1979; Perrett et al. 1982); that IT neurons use sparse distributed encoding for face identity (Baylis et al. 1985; Rolls, Treves, Tovee, Panzeri 1997c) with relatively independent information provided by populations of neurons (Rolls, Treves, Tovee 1997b; Treves et al. 1999; Rolls and Treves 2011); that feature combinations in the correct spatial position encode faces and objects (Perrett et al. 1982; Desimone et al. 1984); and that IT neurons have representations of objects that are invariant with respect to transforms including retinal position (Gross et al. 1985; Tovee et al. 1994), size and contrast (Rolls and Baylis 1986), spatial frequency (Rolls et al. 1985; Rolls et al. 1987), and in some cases to view (Hasselmo, Rolls, Baylis, Nalwa 1989b; Booth and Rolls 1998). For natural vision, in complex natural scenes IT neurons respond primarily to the object being fixated (Sheinberg and Logothetis 2001; Rolls et al. 2003; Aggelopoulos and Rolls 2005) by reducing their receptive field size (Rolls et al. 2003), which simplifies the interpretation of the output of IT by structures such as the orbitofrontal cortex, which implements object-reward association learning (Thorpe et al. 1983; Rolls et al. 1996; Rolls 2019a, 2019b) and the hippocampal system, which implements object-scene location learning (Rolls et al. 2005; Rolls and Xiang 2006; Rolls 2022a). The "what" information to the hippocampal memory system (via TF and in some cases perirhinal or entorhinal cortex) is tapped from this ventrolateral object/face system from the FFC, PH, PHT, TE2p, TE1p, TE2a, and TGd (Figs. 1–3). Moreover, it was discovered that IT neurons can learn rapidly to represent new objects without disturbing representations of previously learned objects (Rolls et al. 1989). Results consistent with these discoveries and principles of operation have been reported (Freiwald et al. 2009; Rust and DiCarlo 2010; Tsao 2014; Freedman 2015; Aparicio et al. 2016; Freiwald 2020; Arcaro and Livingstone 2021).

The hierarchical organization of the connectivity of the Ventrolateral Visual Stream shown schematically in Fig. 6 provides an architecture that with convergence from stage to stages allows features to be combined across larger receptive fields from stage to stage to produce, using competitive learning, neurons that become specialized with sparse distributed encoding to represent different objects and faces (Rolls 1992, 2021a). Invariances such as position, size and view can be built into the neuronal responses by using a local synaptic learning rule in the competitive network that enables these properties of objects, which tend to be invariant over short time epochs of 1—several s, to be learned by the neurons (Rolls 1992, 2021a). This unsupervised self-organizing learning system with only local synaptic learning rules has been built into a model, VisNet, that shows how this learning can take place (Rolls 1992; Wallis and Rolls 1997; Elliffe et al. 2002; Stringer and Rolls 2002; Perry et al. 2006; Stringer et al. 2007; Rolls 2021a; Rolls 2021b). A similar approach has been developed by others (Wiskott and Sejnowski 2002; Wyss et al. 2006; Franzius et al. 2007). A very different approach using deep convolution networks (Cadieu et al. 2014; Yamins et al. 2014; Rajalingham et al. 2018) is biologically implausible, because in the brain there is no teacher for each output neuron, and errors between the firing rate of each output neuron and its teacher's instruction cannot be used to calculate for every synapse at every earlier stage of the hierarchy and then backpropagated back to correct every one of those synaptic strengths (Rolls 2021a, 2021b). Further, top–down processes such as memory recall (Rolls and Treves 1994; Treves and Rolls 1994; Rolls 2021a) and top–down attention (Deco and Rolls 2004, 2005; Rolls 2021a) can be implemented biologically plausibly by the backprojection effective connectivities found in the system (Figs. 1–3 and 6), and that functionality is likely to be inconsistent with error backpropagation.

A Ventromedial Visual Cortical Stream to the parahippocampal gyrus for scene representations based on spatial combinations of visual features. This is a ventral "where" system

The effective connectivity described here leads to the concept of a Ventromedial Visual Cortical Stream that builds representations of visual scenes in the parahippocampal gyrus PHA1—PHA3.

Figure 7 summarizes key parts of the Ventromedial Visual Cortical Stream, which reaches the parahippocampal gyrus PHA1—PHA3 regions via ventromedial (VMV) and ventral visual complex (VVC) regions. Visual scenes are represented in the anterior parts of VMV and the posterior parts of PHA1—PHA3 (Sulpizio et al. 2020) in what is the parahippocampal scene area (PSA) (sometimes called the parahippocampal place area, PPA (Epstein and Kanwisher 1998; Epstein 2005, 2008; Epstein and Julian 2013; Kamps et al. 2016; Epstein and Baker 2019; Sulpizio et al. 2020; Natu et al. 2021)). It is proposed that scene representations are built using combinations of ventral visual stream features that when overlapping in space are locked together by associative learning and can form a continuous attractor network to encode a visual scene (Rolls and Stringer 2005; Stringer et al. 2005; Rolls et al. 2008; Rolls, Deco, et al. 2022a) using spatial view cells (Rolls, Robertson, et al. 1997a; Robertson et al. 1998; Rolls et al. 1998; Georges-François et al. 1999; Wirth et al. 2017; Rolls and Wirth 2018; Tsitsiklis et al. 2020;

Rolls 2022a, 2022b) in the parahippocampal scene (or place) area referred to above, which in turn connects to the hippocampus to provide the "where" component of episodic memory (Rolls, Deco, et al. 2022a, 2022d). In this "Ventromedial Visual Cortical Stream" pathway there is effective connectivity from V1 > V2 > V3 > V4. Then V2, V3 and V4 have effective connectivity to the VMV regions, which in turn have effective connectivity to PHA1–3, which in turn have effective connectivity directed to the hippocampal system (Fig. 7, green arrows) (Rolls, Deco, et al. 2022b). In addition, V2 has effective connectivity to the transitional visual areas DVT and the ProStriate region (ProS), which in humans are where in the HCP-MMP atlas (Glasser, Coalson, et al. 2016a; Huang et al. 2022) the retrosplenial place area is located (Sulpizio et al. 2020); and these regions in turn have effective connectivity to the PHA parahippocampal regions (Fig. 7) (Rolls, Deco, et al. 2022b). In humans, the occipital place area OPA is located in V3CD, V3B, and IP0 (Sulpizio et al. 2020).

The green arrows in Fig. 7 shows how the Ventromedial Visual Cortical Stream provides "where" input about locations in scenes to the hippocampal memory system from the parahippocampal gyrus PHA1-PHA3 regions (which correspond to TH in macaques). This connectivity to the hippocampal scene system is considered further elsewhere (Rolls 2022a, 2022b; Rolls, Deco, et al. 2022a, 2022d).

It is proposed below that a contribution of the dorsal visual stream to scene processing is to provide idiothetic update of the spatial view representations that are in the parahippocampal scene area in PHA1–3/VMV1–3.

Inferior cortex in the Superior Temporal Sulcus: a system for multimodal semantic representations including visual object information

One output of the Ventrolateral Visual Cortical Stream for object and face information is to the cortex in the inferior parts of the Superior Temporal Sulcus (STS), STSva, and STSvp (Rolls, Deco, et al. 2022c). These inferior cortical regions in the STS have been identified by a community analysis as part of a ventral temporal lobe semantic system involved in language (Rolls, Deco, et al. 2022c). The visual inputs to regions STSva and STSvp in this ventral STS semantic system are described here. The visual inputs to these inferior STS regions STSva and STSvp are shown in Fig. 8, and come from TE1a, TE1m, TE2a, TGd, TGv, and PGi. Other connectivities shown with green arrows in Fig. 8 are with the memory-related parts of the posterior cingulate cortex (31pd and 31pv); and from the vmPFC (10v and 10r) (see Fig. 1). STSva and STSvp have connectivity directed towards Broca's area 44 and 45, and related areas (47s, 47l), and to the superior frontal language region SFL (Figs. 1 and 2) (Rolls, Deco, et al. 2022c). This "inferior STS cortex semantic network," for which the visual input is described here, is described in more detail for the same participants elsewhere (Rolls, Deco, et al. 2022c).

This inferior (/ventral) STS cortex network that includes STSva and STSvp is considered to be separate from the superior (/dorsal) STS cortex network described below that includes STSda and STSdp because these regions fall into different semantic connectivity networks as shown by a community analysis (Rolls, Deco, et al. 2022c). The inferior network is likely to be more involved in invariant object and face identity representations for static visual stimuli of the type represented in the inferior temporal visual cortex, whereas the superior regions are more likely to be involved in responses to face expression and visual motion including that which can be combined with auditory stimuli such as the sight and sound of a vocalization (Baylis et al. 1987; Hasselmo, Rolls, Baylis 1989a; Hasselmo, Rolls, Baylis, Nalwa 1989b; Rolls 2021a).

A Dorsal Visual Cortical Stream for visual motion leading to the intraparietal visual areas, and then to parietal area 7 regions for actions in space, with visual motion outputs to the superior STS semantic system. This system includes a dorsal "where"/action system in which idiothetic update of spatial representations is performed

The Dorsal Visual Cortical Stream pathways described here lead via dorsal visual system cortical regions to regions in the intraparietal sulcus and parietal cortex area 7. The details of the effective connectivity of the human dorsal visual Stream are provided in Figs. 1–3 and are described in the Results, and Fig. 9 shows a schematic overview. Effective connectivity from regions such as V2, V3, V3A and V3B, V6A, and V7 reach the MT+ complex regions (FST, LO1, LO2, LO3, MST, MT, PH, V3CD, and V4t) (Figs. 1–3). The MT+ complex regions then have effective connectivity to the intraparietal regions (AIP, LIPd, LIPv, MIP, VIP IP0, IP1 and IP2), which in turn have effective connectivity to the area 7 regions (Figs. 1–3). Interestingly, there are some inputs to this dorsal visual Stream from Ventrolateral Visual Stream regions such as FFC and TE2p, and these are shown with dashed lines in Fig. 9.

V3A and V6 are motion-sensitive areas that project to the MT+ Complex regions in what is described in macaques as a dorsolateral visual stream, which eventually reaches the cortex in the superior temporal sulcus (Galletti and Fattori 2018). V6 responds to coherent optic flow stimuli and may thus be useful in egomotion (Sulpizio et al. 2020). In macaques, V6 may also project to V6A, which is involved in the fast control of prehension and in selecting appropriate postures during reach to grasp behaviors (Monaco et al. 2011; Pitzalis et al. 2013; Pitzalis et al. 2015; Tosoni et al. 2015). V6A then projects to what is described as a dorsomedial visual stream directed towards the intraparietal areas such as MIP, which are also involved in reach to grasp behavior (Galletti and Fattori 2018). Neurons in V6A and VIP are invariant with respect to eye position, that is, they can respond in head-based coordinates (Galletti and Fattori 2018). Coordinate transforms of this type

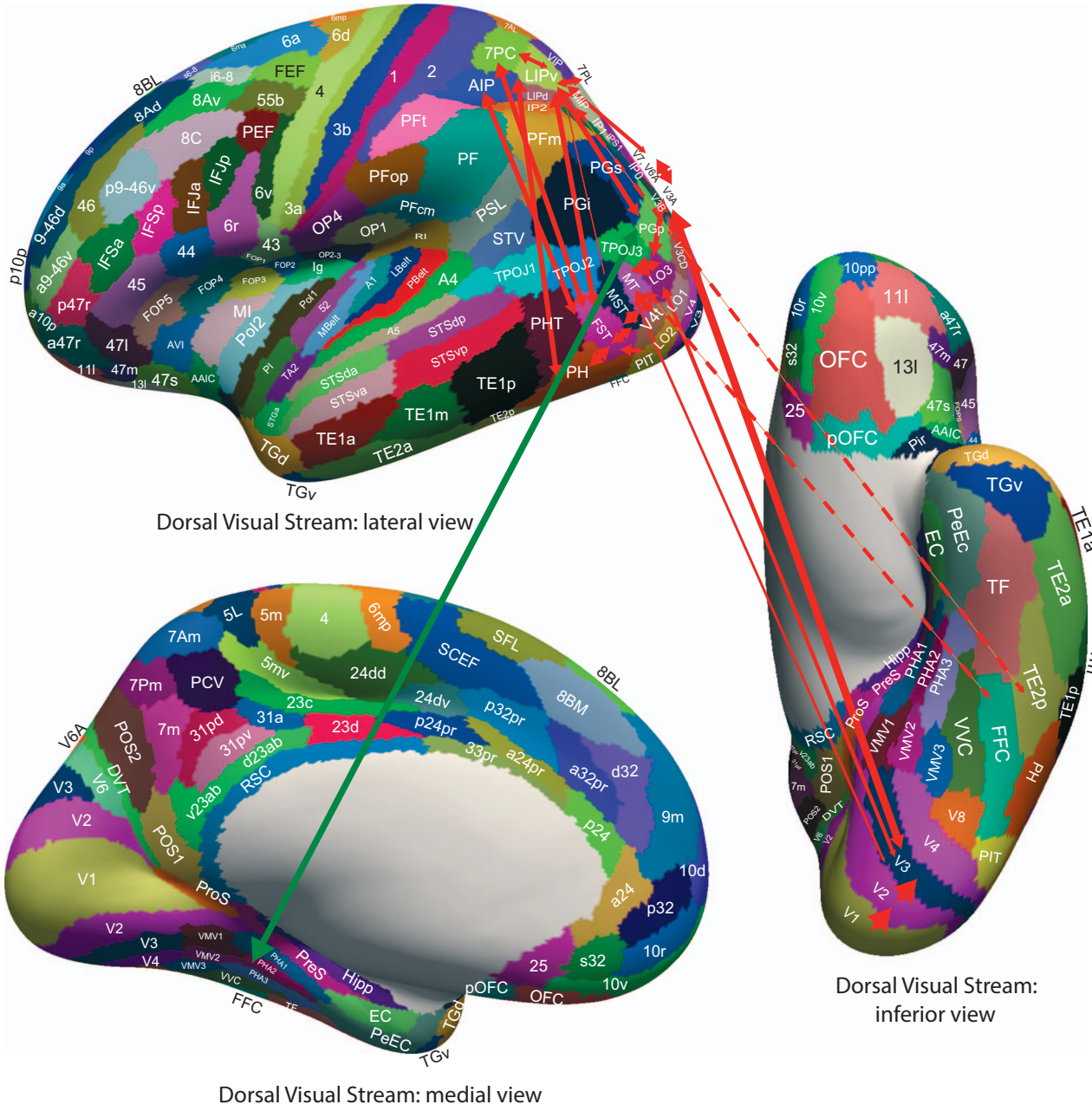

Fig. 9. Effective connectivity of the human dorsal visual cortical stream, which reaches (partly via V3, V3A and LO3) the MT+ complex regions (FST, LO1, LO2, LO3, MST, MT, PH, V3CD and V4t), and then the intraparietal regions (AIP, LIPd, LIPv, MIP, VIP IP0, IP1 and IP2) and then the area 7 regions: Schematic overview. Connectivity to the inferior parietal cortex region PGp, which in turn has effective connectivity to the parahippocampal scene area in PHA1–3 (Rolls, Deco, et al. 2022a) is shown. Inputs to this stream from ventral stream regions such as FFC and TE2p are shown with dashed lines.

can be implemented by gain modulation (Salinas and Sejnowski 2001) (in which for example eye direction modulates retinotopic position), which is greatly helped by slow learning to capture the statistical continuities of an object in a fixed position relative to the head when the eyes move (Rolls 2020). The same principle can be extended to account for the next transform to allocentric direction in space, and then to a further transform to allocentric location in space independently of the place where the individual is located (Rolls 2020), as represented in the parahippocampal gyrus and hippocampus by spatial view cells (Rolls 2022a). This dorsomedial part of the dorsal visual system provides for idiothetic (self-motion) update of allocentric spatial representations of the type provided by for example primate spatial view cells (Robertson et al. 1998), and is a key computation performed in the dorsal visual "where" system enabling idiothetic update of the ventromedial "where" visual cortical Stream for building scene representations in the VMV and PHA1-PHA3 parahippocampal areas described above (see Fig. 9). These scene representations are likely to be involved in human navigation from viewed location to viewed location, which is frequently how navigational instructions are provided in humans (Rolls 2021d). The idiothetic update of scene representations is likely to be important for navigation if the view

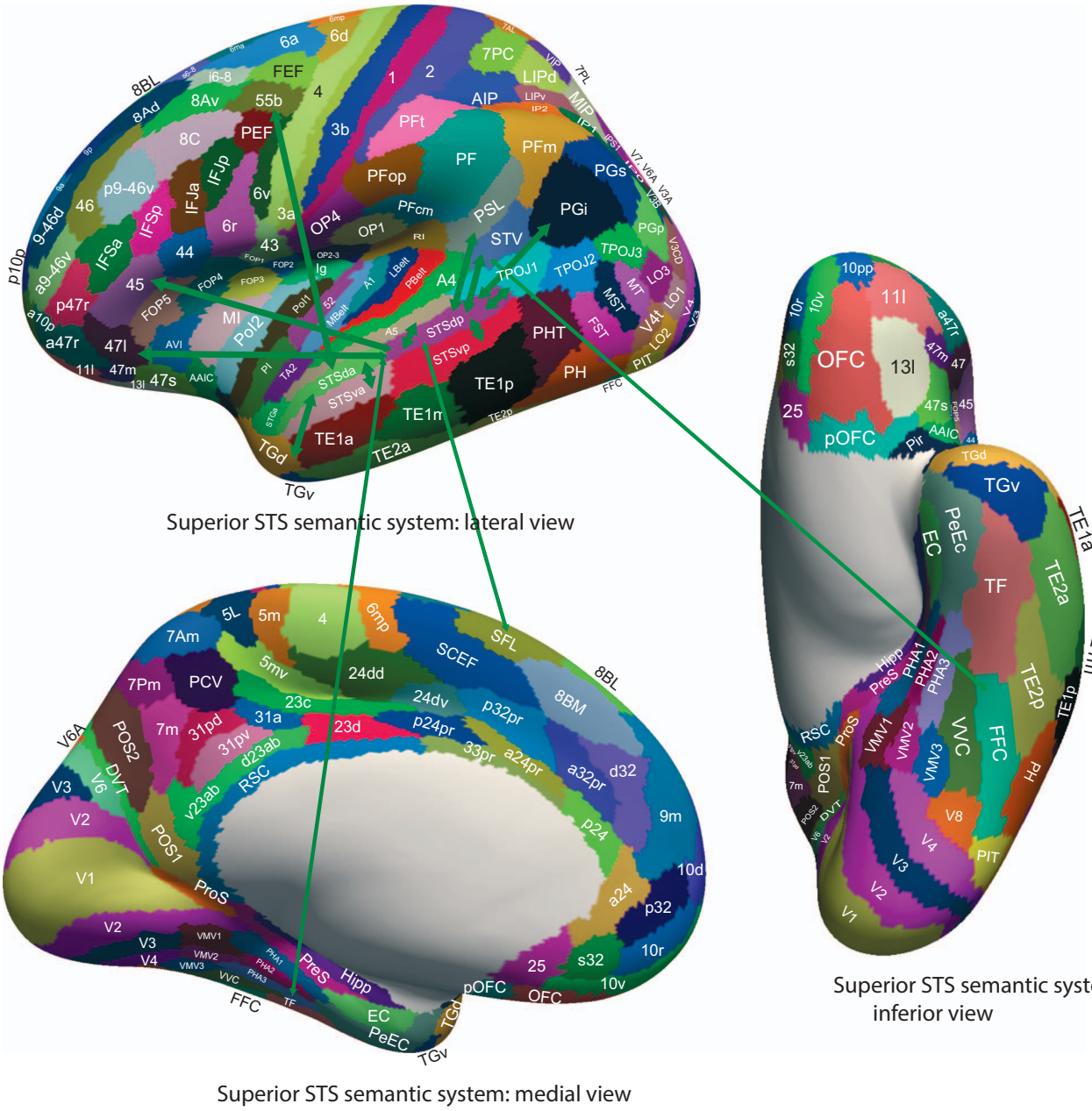

Fig. 10. Superior STS semantic system in STSda and STSdp: schematic overview. Visual inputs for moving visual stimuli/objects reach STSdp from PGi. Visual inputs also reach STSdp from the superior temporal visual area, which receives from FFC. STSda and STSdp also have connectivity from STSva and STSvp, which have strong connectivity with the Ventrolateral Visual Stream (Fig. 6). STSda and STSdp also receive auditory effective connectivity from A5. STSdp has connectivity directed towards Broca's area 44 and 45, and related areas (47l), and to the PeriSylvian language region PSL and to the superior frontal language region SFL (Figs. 1 and 2) (Rolls, Deco, et al. 2022c).

details are temporarily obscured, or in the dark (Rolls 2021d, 2022a).

MT+ complex regions (FST, LO1, LO2, LO3, MST, MT, PH, V3CD, and V4t)

In macaques, MT neurons compute global motion aided by their receptive fields being about 10 times larger than V1 neurons (Newsome et al. 1989; Zaharia et al. 2019). In MST, the receptive fields are larger (e.g. 40°), and some neurons respond to more complex types of motion such as expanding optic flow consistent with moving forwards in an environment, or rotation of the optic flow in a clockwise vs anticlockwise direction, and therefore useful in analyzing self-motion or the motion of an object, disparity may be encoded, and vestibular inputs related to self-motion can influence some neurons (Wild and Treue 2021).

In a unifying hypothesis with the design of the ventral cortical visual system about how these types of encoded motion might be computed, Rolls and Stringer (2006) proposed that the dorsal visual system uses a hierarchical feedforward network architecture (V1, V2, MT, MST, parietal cortex) with training of the synaptic connections with a short-term memory trace associative synaptic

modification rule to compute what is invariant at each stage by utilizing the temporal continuity inherent in the statistics of the visual inputs. An example might be clockwise rotation of an object as it moved across the visual field, or looming of an object. It was demonstrated with simulations that the proposal is feasible computationally, in that invariant representations of the motion flow fields produced by objects self-organize in the higher Layers of the architecture. The computational architecture produces invariant representations of the motion flow fields produced by global in-plane motion of an object, in-plane rotational motion, and receding vs looming of the object. The same principle (Rolls and Stringer 2006) can account for the responses of neurons further on in the system in the cortex in the superior temporal sulcus, which it was discovered can respond to object-based rotation about a principal axis, for example to a head rotating clockwise, invariantly with respect to whether the head was upright or inverted (Hasselmo, Rolls, Baylis, Nalwa 1989b).

Intraparietal sulcus posterior parietal cortex, regions (AIP, LIPd, LIPv, MIP, VIP; with IPO, IP1, and IP2)

Neurons in macaques in area VIP represent the direction and speed of visual motion (Colby et al. 1993), and may be useful in for example tracking moving visual stimuli, and encoding optic flow, which can be useful in assessing self-motion and thereby in navigation. These neurons do not respond in relation to saccades. Neurons in macaques in LIP are active in visual, attentional and saccadic processing (Gnadt and Andersen 1988; Colby et al. 1996; Munuera and Duhamel 2020). The ventral part of LIP (LIPv) has strong connections with two oculomotor centers, the frontal eye field and the deep layers of the superior colliculus, and may be especially involved in the generation of saccades (Chen et al. 2016). The dorsal part (LIPd) may be more involved in visual processing, responding for example to visual targets for saccades (Chen et al. 2016). Neurons in MIP (which may be the parietal reach region, PRR (Connolly et al. 2003)) are related to arm movement preparation and execution (Prado et al. 2005; Filimon et al. 2009; Cavina-Pratesi et al. 2010; Gallivan et al. 2011; Passarelli et al. 2021). They are implicated in the sensory-to-motor transformations required for reaching towards visually defined targets (Gamberini et al. 2020). AIP is activated by grasping objects, for which shaping of the hand based on the visual properties of objects is needed (Culham et al. 2003, 2006).

As shown in Fig. 1, these regions have strong effective connectivity from early visual cortical areas including from several MT+ complex visual regions in which neurons respond to global optic flow (MST, FST, PH, and V3CD), intraparietal sulcus area 1 (IPS1), V3B, V6A (which is a visuo-motor region involved in grasping seen objects (Gamberini et al. 2020)), V7, and superior parietal area 7 regions involved in visuo-motor actions. These intraparietal regions also receive in humans from ventral stream visual cortical areas including the fusiform face cortex (FFC), from inferior temporal cortex regions PIT, PHT, TE1p and TE2p (Fig. 1). These ventral stream regions are likely to bring shape/visual form information to the intraparietal cortex regions important in shaping the hand to grasp and manipulate objects and tools. Consistent with this, neurons in regions such as AIP in macaques can respond to 2D and 3D shape information, which could be helpful in tool use (Kastner et al. 2017). These intraparietal and also area 7 regions may provide information to the inferior parietal cortex regions such as PFt, PF, and PGi that have developed so greatly in humans and that are involved in human tool use (Rolls, Deco, et al. 2022a). These intraparietal regions also have connectivity with the inferior frontal gyrus and with the dorsolateral prefrontal cortex (especially 46, 8C, a9-46, i6-8, and p9-46v), which are likely to be important when there is a delay between the visual input and when the action can be performed (Funahashi et al. 1989). These connectivities are stronger to these prefrontal areas (Fig. 3), as is appropriate for the operation of short-term memory systems so that the memory does not dominate sensory inputs (Rolls 2016, 2021a). There is also connectivity directed towards the parahippocampal TH cortex (PHA3), which may be useful in providing information about visuo-motor actions to the hippocampal memory system. There is also connectivity with the frontal pole p10p, which is likely to be important when sequencing and planning is involved in actions (Shallice and Burgess 1996; Gilbert and Burgess 2008; Shallice and Cipolotti 2018). The connectivity from the intraparietal areas is strongly towards premotor cortical areas including especially 6a, and to the frontal eye field FEF and prefrontal eye field PEF (from especially AIP, LIPd, LIPv, and VIP) (Fig. 3), which provides action-related outputs from these visuo-motor intraparietal regions. There is also connectivity especially for IP1 and IP2 from the orbitofrontal cortex (medial regions, 11 and OFC), which may provide reward feedback (Rolls 2019a, 2019b) of potential utility in learning whether actions made are correct, and with the frontal pole. There is also connectivity with inferior parietal regions including PGp and PGs, with PGp having effective connectivity to the parahippocampal scene area PHA1–3 to provide, it is proposed here, for idiothetic update of parahippocampal and hippocampal spatial view representations (Rolls 2022a; Rolls, Deco, et al. 2022a). Interestingly, this intraparietal part of the parietal cortex has relatively little effective connectivity with the posterior or anterior (or mid) cingulate cortex (Figs. 1–3). The connectivity from MT+ regions such as MT and MST to intraparietal regions from auditory cortical regions such as A4 and A5, and from somatosensory regions such as 5L and 5m (Fig. 1), provides a basis for the auditory and somatosensory responses evident is some macaque intraparietal neurons that also respond to visual stimuli (Kastner et al. 2017).

The functional connectivity is largely consistent (Fig. 4), but indicates more interactions with early visual cortical areas; with somatosensory/premotor

areas; with the hippocampal system; with TE1p and TE2p, with posterior cingulate including DVT; and with supragenual anterior cingulate 33pr and p24pr (Rolls, Deco, et al. 2022e). The diffusion tractography (Fig. 5) is also consistent, but suggests in addition connections with auditory cortex that may be useful in orienting gaze towards sounds.

The intraparietal cortical regions in humans thus are likely in terms of their connectivity (Figs. 1–5) to perform visuomotor functions (without substantial somatosensory processing unlike area 7 regions), and the extensive research on these regions in macaques provides a guide to their functions in humans, including the control of eye movements to acquire and track visual stimuli given the outputs to the FEF and PEF. There are also outputs to regions 6a and 6r that might produce head and body movements to help stabilize images for the visual system. The output to the posterior inferior temporal visual cortex PHT is of interest, and might be involved in the stabilization of images for processing in later parts of the ventral visual system.

Area 7 regions

Area 7 regions in the posterior parietal cortex receive from the intraparietal areas, and are involved in actions in space, and their connectivity in humans is not considered here as it has been described and discussed elsewhere (Rolls, Deco, et al. 2022a).

Superior cortex in the Superior Temporal Sulcus: a system for multimodal semantic representations including visual motion, auditory, and somatosensory information

In the superior part of the cortex in the Superior Temporal Sulcus (STS), STSda, and STSdp have been identified by a community analysis as part of a superior temporal lobe semantic system involved in language (Rolls, Deco, et al. 2022c). The visual inputs to regions STSda and STSdp in this superior STS semantic system are described here. Visual inputs reach STSdp from PGi (Figs. 1–3 and 10), and provide a route for moving visual stimuli/objects analyzed in the parietal cortex to reach STS regions (Rolls, Deco, et al. 2022a). Visual inputs also reach STSdp from the superior temporal visual (STV) region, which receives from both MT and FFC (Figs. 1 and 10), and which as described below could contribute to the neuronal activity in the cortex in the STS, which has been shown to respond to moving heads, faces and objects in macaques (Hasselmo, Rolls, Baylis 1989a; Hasselmo, Rolls, Baylis, Nalwa 1989b). STSda and STSdp also have connectivity from STSva and STSvp, which have strong connectivity with the Ventrolateral Visual Stream (Fig. 8 and 10). STSda and STSdp also receive auditory effective connectivity from A5 (Figs. 1–3 and 10). STSdp has connectivity directed towards Broca's area 44 and 45, and related areas (47l), and to the perisylvian language region PSL and to the superior frontal language region SFL (Figs. 1 and 2) (Rolls, Deco, et al. 2022c).

This "superior STS cortex system" thus enables multimodal representations including visual, auditory, and probably also somatosensory via PGi, to gain access to the language system. This is a major output of cortical visual processing for use in language, described in more detail elsewhere (Rolls, Deco, et al. 2022c). There is also a link via TF to the hippocampal memory system (Fig. 10).

Discoveries in macaques provide an indication for what is represented in these STS regions. It was discovered that single neurons in the macaque STS respond to face expression and also to face and head movement to encode the social relevance of stimuli (Hasselmo, Rolls, Baylis 1989a; Hasselmo, Rolls, Baylis, Nalwa 1989b). For example, a neuron might respond to closing of the eyes, or to turning of the head away from facing the viewer, both of which break social contact (Hasselmo, Rolls, Baylis 1989a; Hasselmo, Rolls, Baylis, Nalwa 1989b). Some neurons respond to the direction of gaze (Perrett et al. 1987). It was found that many of the neurons in the STS respond only or much better to moving faces or objects (Hasselmo, Rolls, Baylis 1989a), whereas in the anterior inferior temporal cortex neurons were discovered that respond well to static visual stimuli, and are tuned for face identity (Perrett et al. 1982; Rolls 1984; Hasselmo, Rolls, Baylis 1989a; Rolls, Treves, Tovee 1997b; Rolls, Treves, Tovee, Panzeri 1997c; Rolls 2000; Rolls and Treves 2011). It has been proposed that PGi, with its inputs from PGs, which has connectivity with superior parietal and intraparietal regions that encode visual motion, is part of this processing stream for socially relevant face-related information (Rolls, Deco, et al. 2022a). Consistent with this, the effective connectivity is stronger from PGi to STS regions (Figs. 1–3). In humans, representations of this type could provide part of the basis for the development of systems to interpret the significance of such stimuli, including theory of mind. Consistent with this proposal, activations in the temporo-parietal junction region are related to theory of mind (Schurz et al. 2017; Buckner and DiNicola 2019; DiNicola et al. 2020). Signals of this type are important in understanding the meaning of seen faces and objects, and indeed evidence about moving objects present in the STS may reach it from PGs and PGi, which in turn receive connectivity from the intraparietal sulcus regions (Rolls, Deco, et al. 2022a) in which neurons respond to visual motion and to grasping objects, which are important in tool use (Maravita and Romano 2018), which is another fundamental aspect of the meaning or semantics of stimuli. We proposed that the cortex in the STS in which neurons respond to moving faces, eyes, etc. and to changing facial expression enables ventral stream "what" information to be combined with dorsal stream motion information to form a third visual stream, and that this could be useful for social functions (Hasselmo, Rolls, Baylis 1989a; Hasselmo, Rolls, Baylis, Nalwa 1989b), especially as this system projects to the orbitofrontal cortex/vmPFC where similar types of neuronal response are found (Rolls et al. 2006). The concept that this STS cortical system is important in social behavior has

recently gained support (Pitcher et al. 2019; Pitcher and Ungerleider 2021). Moreover, neurons can respond to auditory stimuli such as vocalization both in the STS regions (Baylis et al. 1987) and in the orbitofrontal cortex (Rolls et al. 2006). The connectivity described here helps to provide a functional framework for the processing streams involved in these types of function.

General discussion

One point to consider is the extent to which the Hopf effective connectivity algorithm when applied to the brain provides evidence that is selective for one link between two brain regions. If the system was linear and consisted of a simple series of connected stages, then the effective connectivity would be the same for all stages. But in practice, the brain is a non-linear system, and each stage has many inputs from different brain regions and many outputs to different brain regions, so the effective connectivity measured between any pair of brain regions may reflect mainly the effective connectivity between that pair of brain regions. In practice, the effective connectivity measured between one pair of brain regions is relatively selective for that stage. For example, FFC has effective connectivity to TE2p, and TE2p has effective connectivity to TE1p, but no effective connectivity was found from FFC to TE1p (Fig. 1). Another example is that A5 has effective connectivity to STSdp, but no earlier stage of auditory processing does (Fig. 1). Another example is that V4 but not V3 or V2 have effective connectivity to PIT (Fig. 1). Another point to emphasize and noted above is that when effective connectivity is found in the top-down direction in a hierarchy, it could reflect top-down modulation of processing at earlier stages for top-down attention (Deco and Rolls 2004, 2005), or it could reflect memory recall (Rolls and Treves 1994; Treves and Rolls 1994), but it does not show that representations of information evident in what neurons respond to are transferred top-down (Rolls 2016, 2021a).

Conclusions

The effective connectivity analyses described here help to identify 5 visual cortical streams in humans.

First, a Ventrolateral Visual "what" Cortical Stream provides for transform invariant representations of object and face identity in the inferior temporal visual cortex (Fig. 6). This stream provides "what" inputs to the hippocampal memory system, and to the orbitofrontal cortex for association with rewards and for use in emotion-related processing. A component of this stream is the visual word-form area, which is at the lateral edge of the FFC, and which appears to compute by similar feature arrangement processes (Dehaene et al. 2005; Dehaene and Cohen 2011; Caffarra et al. 2021; Yeatman and White 2021) as object and face representations (Rolls 2016, 2021a, 2021b).

Second a Ventromedial Visual "where" cortical stream represents scenes in the VMV and parahippocampal PHA1-PHA3 regions (Fig. 7), probably again using visual features locked together in a particular spatial arrangement using slow learning (Rolls 2021b). A property of these first two visual streams is that large scale representations (of scenes) are found medially in VMV and PHA1-PHA3 regions, with objects and faces more laterally in FFC, and words at the lateral edge of FFC. The computations may be similar, but for different scales of input.

Third, an inferior STS cortex semantic stream involving STSva and STSvp receives visual inputs from the ventrolateral "what" visual cortical stream, and combines this with visual and related inputs from the inferior parietal cortex PGi and with reward value/emotional inputs from the orbitofrontal cortex/vmPFC system (Rolls, Deco, et al. 2022e) (Fig. 8) to build multimodal semantic representations (Rolls, Deco, et al. 2022c). This system has effective connectivity directed to Broca's area, where especially in 44 there is evidence that syntax is implemented (Friederici et al. 2017), and to the superior frontal language area (SFL).

Fourth, a dorsal visual cortical stream has connectivity to MT+ regions (e.g. MT and MST), which in turn connect to intraparietal regions (Fig. 9). This system specializes in the analysis of visual motion and its use for many functions, including eye movement control, the perception of moving objects including faces (in the STS), optic flow useful for navigation, prehension and the control of grasping, and coordinate transforms from retinal to head-based and then allocentric representations to form spatial representations that are of locations in space independent of eye position, head direction, and even for spatial view cells of the place where the individual is located (Rolls 2020). It is thus proposed that this dorsal visual cortical stream performs the idiothetic update of spatial view or scene representations in the Ventromedial Visual Cortical Stream in the VMV and PHA parahippocampal regions. (It has been discovered that these spatial scene representations implemented by spatial view cells in the parahippocampal gyrus and hippocampus are updated by idiothetic inputs (Robertson et al. 1998).)

Fifth, a superior STS cortex semantic Stream receives visual inputs from the ventral STS cortex semantic system, from inferior parietal PGi, and from FFC and MT via the superior temporal visual region (STV) (Fig. 10), and also receives auditory input from A5. Body image and tactile information may also reach this region via PGi (Rolls, Deco, et al. 2022a). Neurons in this region in macaques respond to face expression, face, head and body movement, and to vocalization, and are likely to important in semantic representations for social behavior, and also for auditory–visual integration (Baylis et al. 1987; Hasselmo, Rolls, Baylis 1989a; Hasselmo, Rolls, Baylis, Nalwa 1989b). This stream has effective connectivity directed to Broca's region 45, and to SFL, and to premotor 55b, which is part of the language output system (Rolls, Deco, et al. 2022c).

Some points of interest in the human connectivity described here are that with the great development of the human inferior parietal cortex, considerable connectivity is found between visual inferior parietal

regions such as PGi and PGs, and the visual temporal lobe regions in the Ventrolateral Visual Stream (e.g. Fig. 6); that Ventrolateral Visual Stream inputs reach the dorsal visual Stream (Fig. 9, dashed lines); and that dorsal visual Stream regions have some connectivity with ventral stream areas, with for example some MT+ Complex regions having effective connectivity with FFC, and V3A and V3B with VMV regions.

Previous understanding of the cortical visual information streams has been founded on research in non-human primates (Perrett et al. 1982; Hasselmo, Rolls, Baylis 1989a; Felleman and Van Essen 1991; Ungerleider 1995; Rolls 2000; Kravitz et al. 2013; Rolls 2021a), supplemented by activation and functional connectivity studies in humans (Ungerleider and Haxby 1994; Van Essen and Glasser 2018; Pitcher and Ungerleider 2021). The present research goes beyond this by estimating causal connectivity between 55 visual cortical regions in the human brain with a multimodal atlas with 360 cortical areas; by identifying 5 cortical visual streams; and by showing how the outputs of these streams are transmitted to brain areas involved in emotion (the orbitofrontal cortex), in episodic memory (the hippocampus), in short-term/working memory (with specializations in different parts of the prefrontal cortex), in actions in space (the intraparietal and area 7 regions with outputs to premotor cortical regions), and in 2 semantic systems, one more inferior in the cortex in the STS for object and face recognition and perception, and the second more superior in the cortex in the STS for visual motion and auditory information that are important in social behavior together probably with tactile and body image representations from parietal regions. Moreover, the use of effective connectivity between all pairs of cortical regions in this research makes this a considerable advance beyond previous research, because effective connectivity measures the strength of physiological effects in both directions between every pair of cortical regions, and this type of causal effect helps to lead to a computational basis for how cortical systems operate (Rolls 2016, 2021a).

Acknowledgements

The neuroimaging data were provided by the Human Connectome Project, WU-Minn Consortium (Principal Investigators: David Van Essen and Kamil Ugurbil; 1U54MH091657) funded by the 16 NIH Institutes and Centers that support the NIH Blueprint for Neuroscience Research; and by the McDonnell Center for Systems Neuroscience at Washington University. Dr Wei Cheng and Shitong Xiang of ISTBI, Fudan University, Shanghai are thanked for parcellating the data into HCP-MMP surface-based space (Glasser, Coalson, et al. 2016a) and reordering it into HCPex order (Huang et al. 2022). Roscoe Hunter of the University of Warwick is thanked for contributing to the description in the Supplementary Material of the Hopf effective connectivity algorithm.

Supplementary material

Supplementary material is available at *Cerebral Cortex* online.

Author contributions

Edmund Rolls designed and performed the research, and wrote the paper. Gustavo Deco provided the effective connectivity algorithm. Chu-Chung Huang performed the diffusion tractography and prepared the brain figures with the HCP-MMP labels. Jianfeng Feng performed the funding acquisition. All authors approved the paper.

Funding

The work was supported by the following grants. Professor JF: National Key R&D Program of China (No. 2019YFA0709502); 111 Project (No. B18015); Shanghai Municipal Science and Technology Major Project (No. 2018SHZDZX01), ZJLab, and Shanghai Center for Brain Science and Brain-Inspired Technology; and National Key R&D Program of China (No. 2018YFC1312904). GD is supported by a Spanish national research project (ref. PID2019-105772GB-I00 MCIU AEI) funded by the Spanish Ministry of Science, Innovation and Universities (MCIU), State Research Agency (AEI); HBP SGA3 Human Brain Project Specific Grant Agreement 3 (grant agreement no. 945539), funded by the EU H2020 FET Flagship program; SGR Research Support Group support (ref. 2017 SGR 1545), funded by the Catalan Agency for Management of University and Research Grants (AGAUR); Neurotwin Digital twins for model-driven non-invasive electrical brain stimulation (grant agreement ID: 101017716) funded by the EU H2020 FET Proactive program; euSNN European School of Network Neuroscience (grant agreement ID: 860563) funded by the EU H2020 MSCA-ITN Innovative Training Networks; CECH The Emerging Human Brain Cluster (Id. 001-P-001682) within the framework of the European Research Development Fund Operational Program of Catalonia 2014–2020; Brain-Connects: Brain Connectivity during Stroke Recovery and Rehabilitation (id. 201725.33) funded by the Fundacio La Marato TV3; Corticity, FLAG¨ERA JTC 2017, (ref. PCI2018–092891) funded by the Spanish Ministry of Science, Innovation and Universities (MCIU), State Research Agency (AEI). The funding sources had no role in the study design; in the collection, analysis and interpretation of data; in the writing of the report; and in the decision to submit the article for publication.

Conflict of interest statement. The authors have no competing interests to declare.

Data and code availability

The data are available at the HCP website http://www.humanconnectome.org/. Code for the Hopf effective

connectivity algorithm is available at https://github.com/decolab/Effective-Connectivity--Hopf.

Ethical permissions

No data were collected as part of the research described here. The data were from the Human Connectome Project, and the WU-Minn HCP Consortium obtained full informed consent from all participants, and research procedures and ethical guidelines were followed in accordance with the Institutional Review Boards (IRB), with details at the HCP website http://www.e.humanconnectom org/

References

Aggelopoulos NC, Rolls ET. Natural scene perception: inferior temporal cortex neurons encode the positions of different objects in the scene. *Eur J Neurosci*. 2005:22(11):2903–2916.

Aparicio PL, Issa EB, DiCarlo JJ. Neurophysiological organization of the middle face patch in macaque inferior temporal cortex. *J Neurosci*. 2016:36(50):12729–12745.

Arcaro MJ, Livingstone MS. On the relationship between maps and domains in inferotemporal cortex. *Nat Rev Neurosci*. 2021:22(9):573–583.

Bajaj S, Adhikari BM, Friston KJ, Dhamala M. Bridging the gap: dynamic causal modeling and granger causality analysis of resting state functional magnetic resonance imaging. *Brain Connect*. 2016:6(8):652–661.

Baker CM, Burks JD, Briggs RG, Conner AK, Glenn CA, Taylor KN, Sali G, McCoy TM, Battiste JD, O'Donoghue DL, et al. A connectomic atlas of the human cerebrum-chapter 7: the lateral parietal lobe. *Oper Neurosurg (Hagerstown)*. 2018a:15(suppl_1):S295–S349.

Baker CM, Burks JD, Briggs RG, Milton CK, Conner AK, Glenn CA, Sali G, McCoy TM, Battiste JD, O'Donoghue DL, et al. A connectomic atlas of the human cerebrum-chapter 6: the temporal lobe. *Oper Neurosurg (Hagerstown)*. 2018b:15(suppl_1):S245–S294.

Baylis GC, Rolls ET, Leonard CM. Selectivity between faces in the responses of a population of neurons in the cortex in the superior temporal sulcus of the monkey. *Brain Res*. 1985:342(1):91–102.

Baylis GC, Rolls ET, Leonard CM. Functional subdivisions of the temporal lobe neocortex. *J Neurosci*. 1987:7(2):330–342.

Booth MCA, Rolls ET. View-invariant representations of familiar objects by neurons in the inferior temporal visual cortex. *Cereb Cortex*. 1998:8(6):510–523.

Buckner RL, DiNicola LM. The brain's default network: updated anatomy, physiology and evolving insights. *Nat Rev Neurosci*. 2019:20(10):593–608.

Cadieu CF, Hong H, Yamins DL, Pinto N, Ardila D, Solomon EA, Majaj NJ, DiCarlo JJ. Deep neural networks rival the representation of primate IT cortex for core visual object recognition. *PLoS Comput Biol*. 2014:10(12):e1003963.

Caffarra S, Karipidis II, Yablonski M, Yeatman JD. Anatomy and physiology of word-selective visual cortex: from visual features to lexical processing. *Brain Struct Funct*. 2021:226(9):3051–3065.

Catani M, Thiebaut de Schotten M. A diffusion tensor imaging tractography atlas for virtual in vivo dissections. *Cortex*. 2008:44(8):1105–1132.

Cavina-Pratesi C, Monaco S, Fattori P, Galletti C, McAdam TD, Quinlan DJ, Goodale MA, Culham JC. Functional magnetic resonance imaging reveals the neural substrates of arm transport and grip formation in reach-to-grasp actions in humans. *J Neurosci*. 2010:30(31):10306–10323.

Chen M, Li B, Guang J, Wei L, Wu S, Liu Y, Zhang M. Two subdivisions of macaque LIP process visual-oculomotor information differently. *Proc Natl Acad Sci U S A*. 2016:113(41):E6263–E6270.

Colby CL, Duhamel JR, Goldberg ME. Ventral intraparietal area of the macaque: anatomic location and visual response properties. *J Neurophysiol*. 1993:69(3):902–914.

Colby CL, Duhamel JR, Goldberg ME. Visual, presaccadic, and cognitive activation of single neurons in monkey lateral intraparietal area. *J Neurophysiol*. 1996:76(5):2841–2852.

Colclough GL, Smith SM, Nichols TE, Winkler AM, Sotiropoulos SN, Glasser MF, Van Essen DC, Woolrich MW. The heritability of multi-modal connectivity in human brain activity. *Elife*. 2017:6:e20178.

Connolly JD, Andersen RA, Goodale MA. FMRI evidence for a 'parietal reach region' in the human brain. *Exp Brain Res*. 2003:153(2):140–145.

Culham JC, Danckert SL, Souza JFXD, Gati JS, Menon RS, Goodale MA. Visually guided grasping produces fMRI activation in dorsal but not ventral stream brain areas. *Exp Brain Res*. 2003:153(2):180–189.

Culham JC, Cavina-Pratesi C, Singhal A. The role of parietal cortex in visuomotor control: what have we learned from neuroimaging? *Neuropsychologia*. 2006:44(13):2668–2684.

Deco G, Rolls ET. A neurodynamical cortical model of visual attention and invariant object recognition. *Vis Res*. 2004:44(6):621–642.

Deco G, Rolls ET. Attention, short-term memory, and action selection: a unifying theory. *Prog Neurobiol*. 2005:76(4):236–256.

Deco G, Cabral J, Woolrich MW, Stevner ABA, van Hartevelt TJ, Kringelbach ML. Single or multiple frequency generators in on-going brain activity: a mechanistic whole-brain model of empirical MEG data. *NeuroImage*. 2017a:152:538–550.

Deco G, Kringelbach ML, Jirsa VK, Ritter P. The dynamics of resting fluctuations in the brain: metastability and its dynamical cortical core. *Sci Rep*. 2017b:7(1):3095.

Deco G, Cruzat J, Cabral J, Tagliazucchi E, Laufs H, Logothetis NK, Kringelbach ML. Awakening: predicting external stimulation to force transitions between different brain states. *Proc Natl Acad Sci*. 2019:116(36):18088–18097.

Deen B, Koldewyn K, Kanwisher N, Saxe R. Functional organization of social perception and cognition in the superior temporal sulcus. *Cereb Cortex*. 2015:25(11):4596–4609.

Dehaene S, Cohen L. The unique role of the visual word form area in reading. *Trends Cogn Sci*. 2011:15(6):254–262.

Dehaene S, Cohen L, Sigman M, Vinckier F. The neural code for written words: a proposal. *Trends Cogn Sci*. 2005:9(7):335–341.

Desimone R, Albright TD, Gross CG, Bruce C. Stimulus-selective properties of inferior temporal neurons in the macaque. *J Neurosci*. 1984:4(8):2051–2062.

Dhollander T, Raffelt D, Connelly A. Unsupervised 3-tissue response function estimation from single-shell or multi-shell diffusion MR data without a co-registered T1 image. *ISMRM Workshop on Breaking the Barriers of Diffusion MRI* 5. 2016.

DiNicola LM, Braga RM, Buckner RL. Parallel distributed networks dissociate episodic and social functions within the individual. *J Neurophysiol*. 2020:123(3):1144–1179.

Elliffe MCM, Rolls ET, Stringer SM. Invariant recognition of feature combinations in the visual system. *Biol Cybern*. 2002:86(1):59–71.

Epstein R. The cortical basis of visual scene processing. *Vis Cogn*. 2005:12(6):954–978.

Epstein RA. Parahippocampal and retrosplenial contributions to human spatial navigation. *Trends Cogn Sci*. 2008:12(10):388–396.

Epstein RA, Baker CI. Scene perception in the human brain. *Annu Rev Vis Sci*. 2019:5(1):373–397.

Epstein RA, Julian JB. Scene areas in humans and macaques. *Neuron*. 2013:79(4):615–617.

Epstein R, Kanwisher N. A cortical representation of the local visual environment. *Nature*. 1998:392(6676):598–601.

Felleman DJ, Van Essen DC. Distributed hierarchical processing in the primate cerebral cortex. *Cereb Cortex*. 1991:1(1):1–47.

Filimon F, Nelson JD, Huang RS, Sereno MI. Multiple parietal reach regions in humans: cortical representations for visual and proprioceptive feedback during on-line reaching. *J Neurosci*. 2009:29(9):2961–2971.

Franzius M, Sprekeler H, Wiskott L. Slowness and sparseness lead to place, head-direction, and spatial-view cells. *PLoS Comput Biol*. 2007:3(8):e166.

Frassle S, Lomakina EI, Razi A, Friston KJ, Buhmann JM, Stephan KE. Regression DCM for fMRI. *NeuroImage*. 2017:155:406–421.

Freedman DJ. Learning-dependent plasticity of visual encoding in inferior temporal cortex. *J Vis*. 2015:15(12):1420.

Freiwald WA. The neural mechanisms of face processing: cells, areas, networks, and models. *Curr Opin Neurobiol*. 2020:60:184–191.

Freiwald WA, Tsao DY, Livingstone MS. A face feature space in the macaque temporal lobe. *Nat Neurosci*. 2009:12(9):1187–1196.

Freyer F, Roberts JA, Becker R, Robinson PA, Ritter P, Breakspear M. Biophysical mechanisms of multistability in resting-state cortical rhythms. *J Neurosci*. 2011:31(17):6353–6361.

Freyer F, Roberts JA, Ritter P, Breakspear M. A canonical model of multistability and scale-invariance in biological systems. *PLoS Comput Biol*. 2012:8(8):e1002634.

Friederici AD, Chomsky N, Berwick RC, Moro A, Bolhuis JJ. Language, mind and brain. *Nat Hum Behav*. 2017:1(10):713–722.

Friston K. Causal modelling and brain connectivity in functional magnetic resonance imaging. *PLoS Biol*. 2009:7(2):e33.

Funahashi S, Bruce CJ, Goldman-Rakic PS. Mnemonic coding of visual space in the monkey's dorsolateral prefrontal cortex. *J Neurophysiol*. 1989:61(2):331–349.

Galletti C, Fattori P. The dorsal visual stream revisited: stable circuits or dynamic pathways? *Cortex*. 2018:98:203–217.

Gallivan JP, Goodale MA. The dorsal "action" pathway. *Handb Clin Neurol*. 2018:151:449–466.

Gallivan JP, McLean A, Culham JC. Neuroimaging reveals enhanced activation in a reach-selective brain area for objects located within participants' typical hand workspaces. *Neuropsychologia*. 2011:49(13):3710–3721.

Gamberini M, Passarelli L, Fattori P, Galletti C. Structural connectivity and functional properties of the macaque superior parietal lobule. *Brain Struct Funct*. 2020:225(4):1349–1367.

Georges-François P, Rolls ET, Robertson RG. Spatial view cells in the primate hippocampus: allocentric view not head direction or eye position or place. *Cereb Cortex*. 1999:9(3):197–212.

Gilbert SJ, Burgess PW. Executive function. *Curr Biol*. 2008:18(3):R110–R114.

Gilson M, Moreno-Bote R, Ponce-Alvarez A, Ritter P, Deco G. Estimation of directed effective connectivity from fMRI functional connectivity hints at asymmetries of cortical connectome. *PLoS Comput Biol*. 2016:12(3):e1004762.

Glasser MF, Sotiropoulos SN, Wilson JA, Coalson TS, Fischl B, Andersson JL, Xu J, Jbabdi S, Webster M, Polimeni JR, et al. The minimal preprocessing pipelines for the human connectome project. *NeuroImage*. 2013:80:105–124.

Glasser MF, Coalson TS, Robinson EC, Hacker CD, Harwell J, Yacoub E, Ugurbil K, Andersson J, Beckmann CF, Jenkinson M, et al. A multi-modal parcellation of human cerebral cortex. *Nature*. 2016a:536(7615):171–178.

Glasser MF, Smith SM, Marcus DS, Andersson JL, Auerbach EJ, Behrens TE, Coalson TS, Harms MP, Jenkinson M, Moeller S, et al. The human connectome Project's neuroimaging approach. *Nat Neurosci*. 2016b:19(9):1175–1187.

Gnadt JW, Andersen RA. Memory related motor planning activity in posterior parietal cortex of macaque. *Exp Brain Res*. 1988:70(1):216–220.

Griffanti L, Salimi-Khorshidi G, Beckmann CF, Auerbach EJ, Douaud G, Sexton CE, Zsoldos E, Ebmeier KP, Filippini N, Mackay CE, et al. ICA-based artefact removal and accelerated fMRI acquisition for improved resting state network imaging. *NeuroImage*. 2014:95:232–247.

Gross CG, Desimone R, Albright TD, Schwartz EL. Inferior temporal cortex and pattern recognition. *Exp Brain Res*. 1985:11:179–201.

Hasselmo ME, Rolls ET, Baylis GC. The role of expression and identity in the face-selective responses of neurons in the temporal visual cortex of the monkey. *Behav Brain Res*. 1989a:32(3):203–218.

Hasselmo ME, Rolls ET, Baylis GC, Nalwa V. Object-centred encoding by face-selective neurons in the cortex in the superior temporal sulcus of the monkey. *Exp Brain Res*. 1989b:75(2):417–429.

Huang C-C, Rolls ET, Hsu C-CH, Feng J, Lin C-P. Extensive cortical connectivity of the human hippocampal memory system: beyond the "what" and "where" dual stream model. *Cereb Cortex*. 2021:31(10):4652–4669.

Huang CC, Rolls ET, Feng J, Lin CP. An extended human connectome project multimodal parcellation atlas of the human cortex and subcortical areas. *Brain Struct Funct*. 2022:227(3):763–778.

Isik L, Koldewyn K, Beeler D, Kanwisher N. Perceiving social interactions in the posterior superior temporal sulcus. *Proc Natl Acad Sci U S A*. 2017:114(43):E9145–E9152.

Jeurissen B, Tournier JD, Dhollander T, Connelly A, Sijbers J. Multi-tissue constrained spherical deconvolution for improved analysis of multi-shell diffusion MRI data. *NeuroImage*. 2014:103:411–426.

Kamps FS, Julian JB, Kubilius J, Kanwisher N, Dilks DD. The occipital place area represents the local elements of scenes. *NeuroImage*. 2016:132:417–424.

Kastner S, Chen Q, Jeong SK, Mruczek REB. A brief comparative review of primate posterior parietal cortex: a novel hypothesis on the human toolmaker. *Neuropsychologia*. 2017:105:123–134.

Kolster H, Peeters R, Orban GA. The retinotopic organization of the human middle temporal area MT/V5 and its cortical neighbors. *J Neurosci*. 2010:30(29):9801–9820.

Kravitz DJ, Saleem KS, Baker CI, Ungerleider LG, Mishkin M. The ventral visual pathway: an expanded neural framework for the processing of object quality. *Trends Cogn Sci*. 2013:17(1):26–49.

Kringelbach ML, Deco G. Brain states and transitions: insights from computational neuroscience. *Cell Rep*. 2020:32(10):108128.

Kringelbach ML, McIntosh AR, Ritter P, Jirsa VK, Deco G. The rediscovery of slowness: exploring the timing of cognition. *Trends Cogn Sci*. 2015:19(10):616–628.

Kuznetsov YA. *Elements of applied bifurcation theory*. New York: Springer Science & Business Media; 2013

Ma Q, Rolls ET, Huang C-C, Cheng W, Feng J. Extensive cortical functional connectivity of the human hippocampal memory system. *Cortex*. 2022:147:83–101.

Maier-Hein KH, Neher PF, Houde JC, Cote MA, Garyfallidis E, Zhong J, Chamberland M, Yeh FC, Lin YC, Ji Q, et al. The challenge of mapping the human connectome based on diffusion tractography. *Nat Commun*. 2017:8(1):1349.

Maravita A, Romano D. The parietal lobe and tool use. *Handb Clin Neurol*. 2018:151:481–498.

Markov NT, Vezoli J, Chameau P, Falchier A, Quilodran R, Huissoud C, Lamy C, Misery P, Giroud P, Ullman S, et al. Anatomy of hierarchy: feedforward and feedback pathways in macaque visual cortex. *J Comp Neurol*. 2014:522(1):225–259.

Milner AD. How do the two visual streams interact with each other? *Exp Brain Res*. 2017:235(5):1297–1308.

Milner AD, Goodale MA. *The visual brain in action*. Oxford: Oxford University Press; 1995

Monaco S, Cavina-Pratesi C, Sedda A, Fattori P, Galletti C, Culham JC. Functional magnetic resonance adaptation reveals the involvement of the dorsomedial stream in hand orientation for grasping. *J Neurophysiol*. 2011:106(5):2248–2263.

Munuera J, Duhamel JR. The role of the posterior parietal cortex in saccadic error processing. *Brain Struct Funct*. 2020:225(2):763–784.

Natu VS, Arcaro MJ, Barnett MA, Gomez J, Livingstone M, Grill-Spector K, Weiner KS. Sulcal depth in the medial ventral temporal cortex predicts the location of a place-selective region in macaques, children, and adults. *Cereb Cortex*. 2021:31(1): 48–61.

Newsome WT, Britten KH, Movshon JA. Neuronal correlates of a perceptual decision. *Nature*. 1989:341(6237):52–54.

Orban GA, Sepe A, Bonini L. Parietal maps of visual signals for bodily action planning. *Brain Struct Funct*. 2021:226(9):2967–2988.

Passarelli L, Gamberini M, Fattori P. The superior parietal lobule of primates: a sensory-motor hub for interaction with the environment. *J Integr Neurosci*. 2021:20(1):157–171.

Perrett DI, Rolls ET, Caan W. Temporal lobe cells of the monkey with visual responses selective for faces. *Neurosci Lett*. 1979:S3:S358.

Perrett DI, Rolls ET, Caan W. Visual neurons responsive to faces in the monkey temporal cortex. *Exp Brain Res*. 1982:47(3): 329–342.

Perrett D, Mistlin A, Chitty A. Visual neurons responsive to faces. *Trends Neurosci*. 1987:10(9):358–364.

Perry G, Rolls ET, Stringer SM. Spatial vs temporal continuity in view invariant visual object recognition learning. *Vis Res*. 2006:46(23): 3994–4006.

Pitcher D, Ungerleider LG. Evidence for a third visual pathway specialized for social perception. *Trends Cogn Sci*. 2021:25(2):100–110.

Pitcher D, Ianni G, Ungerleider LG. A functional dissociation of face-, body- and scene-selective brain areas based on their response to moving and static stimuli. *Sci Rep*. 2019:9(1):8242.

Pitzalis S, Sereno MI, Committeri G, Fattori P, Galati G, Tosoni A, Galletti C. The human homologue of macaque area V6A. *NeuroImage*. 2013:82:517–530.

Pitzalis S, Fattori P, Galletti C. The human cortical areas V6 and V6A. *Vis Neurosci*. 2015:32:E007.

Power JD, Cohen AL, Nelson SM, Wig GS, Barnes KA, Church JA, Vogel AC, Laumann TO, Miezin FM, Schlaggar BL, et al. Functional network organization of the human brain. *Neuron*. 2011:72(4): 665–678.

Prado J, Clavagnier S, Otzenberger H, Scheiber C, Kennedy H, Perenin MT. Two cortical systems for reaching in central and peripheral vision. *Neuron*. 2005:48(5):849–858.

Rajalingham R, Issa EB, Bashivan P, Kar K, Schmidt K, DiCarlo JJ. Large-scale, high-resolution comparison of the core visual object recognition behavior of humans, monkeys, and state-of-the-art deep artificial neural networks. *J Neurosci*. 2018:38(33): 7255–7269.

Razi A, Seghier ML, Zhou Y, McColgan P, Zeidman P, Park HJ, Sporns O, Rees G, Friston KJ. Large-scale DCMs for resting-state fMRI. *Netw Neurosci*. 2017:1(3):222–241.

Robertson RG, Rolls ET, Georges-François P. Spatial view cells in the primate hippocampus: effects of removal of view details. *J Neurophysiol*. 1998:79(3):1145–1156.

Rolls ET. Neurons in the cortex of the temporal lobe and in the amygdala of the monkey with responses selective for faces. *Hum Neurobiol*. 1984:3(4):209–222.

Rolls ET. Neurophysiological mechanisms underlying face processing within and beyond the temporal cortical visual areas. *Philos Trans R Soc Lond B*. 1992:335(1273):11–21.

Rolls ET. Functions of the primate temporal lobe cortical visual areas in invariant visual object and face recognition. *Neuron*. 2000:27(2): 205–218.

Rolls ET. *Cerebral cortex: principles of operation*. Oxford: Oxford University Press; 2016

Rolls ET. *The orbitofrontal cortex*. Oxford: Oxford University Press; 2019a

Rolls ET. The orbitofrontal cortex and emotion in health and disease, including depression. *Neuropsychologia*. 2019b:128:14–43.

Rolls ET. Spatial coordinate transforms linking the allocentric hippocampal and egocentric parietal primate brain systems for memory, action in space, and navigation. *Hippocampus*. 2020:30(4): 332–353.

Rolls ET. *Brain computations: what and how*. Oxford: Oxford University Press; 2021a

Rolls ET. Learning invariant object and spatial view representations in the brain using slow unsupervised learning. *Front Comput Neurosci*. 2021b:15:686239.

Rolls ET. Mind causality: a computational neuroscience approach. *Front Comput Neurosci*. 2021c:15:70505.

Rolls ET. Neurons including hippocampal spatial view cells, and navigation in primates including humans. *Hippocampus*. 2021d:31(6): 593–611.

Rolls ET. Hippocampal spatial view cells for memory and navigation, and their underlying connectivity in humans. *Hippocampus*. 2022a: in revision.

Rolls ET. The hippocampus, ventromedial-prefrontal cortex, and episodic and semantic memory. *Prog Neurobiol*. 2022b: in revision.

Rolls ET, Baylis GC. Size and contrast have only small effects on the responses to faces of neurons in the cortex of the superior temporal sulcus of the monkey. *Exp Brain Res*. 1986:65(1): 38–48.

Rolls ET, Stringer SM. Spatial view cells in the hippocampus, and their idiothetic update based on place and head direction. *Neural Netw*. 2005:18(9):1229–1241.

Rolls ET, Stringer SM. Invariant global motion recognition in the dorsal visual system: a unifying theory. *Neural Comput*. 2006:19(1): 139–169.

Rolls ET, Treves A. Neural networks in the brain involved in memory and recall. *Prog Brain Res*. 1994:102:335–341.

Rolls ET, Treves A. The neuronal encoding of information in the brain. *Prog Neurobiol*. 2011:95(3):448–490.

Rolls ET, Wirth S. Spatial representations in the primate hippocampus, and their functions in memory and navigation. *Prog Neurobiol*. 2018:171:90–113.

Rolls ET, Xiang J-Z. Spatial view cells in the primate hippocampus, and memory recall. *Rev Neurosci*. 2006:17(1–2):175–200.

Rolls ET, Judge SJ, Sanghera M. Activity of neurones in the inferotemporal cortex of the alert monkey. *Brain Res*. 1977:130(2): 229–238.

Rolls ET, Baylis GC, Leonard CM. Role of low and high spatial frequencies in the face-selective responses of neurons in the cortex in the superior temporal sulcus in the monkey. *Vis Res*. 1985:25(8): 1021–1035.

Rolls ET, Baylis GC, Hasselmo ME. The responses of neurons in the cortex in the superior temporal sulcus of the monkey to band-pass spatial frequency filtered faces. *Vis Res*. 1987:27(3):311–326.

Rolls ET, Baylis GC, Hasselmo ME, Nalwa V. The effect of learning on the face selective responses of neurons in the cortex in the superior temporal sulcus of the monkey. *Exp Brain Res*. 1989:76(1):153–164.

Rolls ET, Critchley HD, Mason R, Wakeman EA. Orbitofrontal cortex neurons: role in olfactory and visual association learning. *J Neurophysiol*. 1996:75(5):1970–1981.

Rolls ET, Robertson RG, Georges-François P. Spatial view cells in the primate hippocampus. *Eur J Neurosci*. 1997a:9(8):1789–1794.

Rolls ET, Treves A, Tovee MJ. The representational capacity of the distributed encoding of information provided by populations of neurons in primate temporal visual cortex. *Exp Brain Res*. 1997b:114(1):149–162.

Rolls ET, Treves A, Tovee MJ, Panzeri S. Information in the neuronal representation of individual stimuli in the primate temporal visual cortex. *J Comput Neurosci*. 1997c:4(4):309–333.

Rolls ET, Treves A, Robertson RG, Georges-François P, Panzeri S. Information about spatial view in an ensemble of primate hippocampal cells. *J Neurophysiol*. 1998:79(4):1797–1813.

Rolls ET, Aggelopoulos NC, Zheng F. The receptive fields of inferior temporal cortex neurons in natural scenes. *J Neurosci*. 2003:23(1):339–348.

Rolls ET, Xiang J-Z, Franco L. Object, space and object-space representations in the primate hippocampus. *J Neurophysiol*. 2005:94(1):833–844.

Rolls ET, Critchley HD, Browning AS, Inoue K. Face-selective and auditory neurons in the primate orbitofrontal cortex. *Exp Brain Res*. 2006:170(1):74–87.

Rolls ET, Tromans J, Stringer SM. Spatial scene representations formed by self-organizing learning in a hippocampal extension of the ventral visual system. *Eur J Neurosci*. 2008:28(10):2116–2127.

Rolls ET, Deco G, Huang C-C, Feng J. The human posterior parietal cortex: effective connectome, and its relation to function. *Cereb Cortex*. 2022a. https://doi.org/10.1093/cercor/bhac1266.

Rolls ET, Deco G, Huang C-C, Feng J. Multiple cortical visual streams in humans. *Cereb Cortex*. 2022b. https://doi.org/10.1093/cercor/bhac276.

Rolls ET, Deco G, Huang C-C, Feng J. The human language effective connectome. *NeuroImage*. 2022c:258:119352.

Rolls ET, Deco G, Huang CC, Feng J. The effective connectivity of the human hippocampal memory system. *Cereb Cortex*. 2022d. https://doi.org/10.1093/cercor/bhab442.

Rolls ET, Deco G, Huang CC, Feng J. The human orbitofrontal cortex, vmPFC, and anterior cingulate cortex effective connectome: emotion, memory, and action. *Cereb Cortex*. 2022e. https://doi.org/10.1093/cercor/bhac070.

Rolls ET, Wirth S, Deco G, Huang C-C, Feng J. The human posterior cingulate, retrosplenial and medial parietal cortex effective connectome, and implications for memory and navigation. *Hum Brain Mapp*. 2022f.

Rust NC, DiCarlo JJ. Selectivity and tolerance ("invariance") both increase as visual information propagates from cortical area V4 to IT. *J Neurosci*. 2010:30(39):12978–12995.

Salimi-Khorshidi G, Douaud G, Beckmann CF, Glasser MF, Griffanti L, Smith SM. Automatic denoising of functional MRI data: combining independent component analysis and hierarchical fusion of classifiers. *NeuroImage*. 2014:90:449–468.

Salinas E, Sejnowski TJ. Gain modulation in the central nervous system: where behavior, neurophysiology, and computation meet. *Neuroscientist*. 2001:7(5):430–440.

Satterthwaite TD, Elliott MA, Gerraty RT, Ruparel K, Loughead J, Calkins ME, Eickhoff SB, Hakonarson H, Gur RC, Gur RE, et al. An improved framework for confound regression and filtering for control of motion artifact in the preprocessing of resting-state functional connectivity data. *NeuroImage*. 2013:64:240–256.

Scheirer J, Ray WS, Hare N. The analysis of ranked data derived from completely randomized factorial designs. *Biometrics*. 1976:32(2):429–434.

Schurz M, Tholen MG, Perner J, Mars RB, Sallet J. Specifying the brain anatomy underlying temporo-parietal junction activations for theory of mind: a review using probabilistic atlases from different imaging modalities. *Hum Brain Mapp*. 2017:38(9):4788–4805.

Shallice T, Burgess P. The domain of supervisory processes and temporal organization of behaviour. *Philos Trans R Soc B*. 1996:351(1346):1405–1412.

Shallice T, Cipolotti L. The prefrontal cortex and neurological impairments of active thought. *Annu Rev Psychol*. 2018:69(1):157–180.

Sheinberg DL, Logothetis NK. Noticing familiar objects in real world scenes: the role of temporal cortical neurons in natural vision. *J Neurosci*. 2001:21(4):1340–1350.

Sinha N. *Non-parametric alternative of 2-way ANOVA (ScheirerRayHare) MATLAB central file exchange*. 2022. https://www.mathworks.com/matlabcentral/fileexchange/96399-non-parametric-alternative-of-96392-way-anova-scheirerrayhare.

Smith SM. Fast robust automated brain extraction. *Hum Brain Mapp*. 2002:17(3):143–155.

Smith SM, Beckmann CF, Andersson J, Auerbach EJ, Bijsterbosch J, Douaud G, Duff E, Feinberg DA, Griffanti L, Harms MP, et al. Resting-state fMRI in the human connectome project. *NeuroImage*. 2013:80:144–168.

Smith RE, Tournier JD, Calamante F, Connelly A. SIFT2: enabling dense quantitative assessment of brain white matter connectivity using streamlines tractography. *NeuroImage*. 2015:119:338–351.

Stringer SM, Rolls ET. Invariant object recognition in the visual system with novel views of 3D objects. *Neural Comput*. 2002:14(11):2585–2596.

Stringer SM, Rolls ET, Trappenberg TP. Self-organizing continuous attractor network models of hippocampal spatial view cells. *Neurobiol Learn Mem*. 2005:83(1):79–92.

Stringer SM, Rolls ET, Tromans J. Invariant object recognition with trace learning and multiple stimuli present during training. *Netw Comput Neural Syst*. 2007:18(2):161–187.

Sulpizio V, Galati G, Fattori P, Galletti C, Pitzalis S. A common neural substrate for processing scenes and egomotion-compatible visual motion. *Brain Struct Funct*. 2020:225(7):2091–2110.

Thorpe SJ, Rolls ET, Maddison S. The orbitofrontal cortex: neuronal activity in the behaving monkey. *Exp Brain Res*. 1983:49(1):93–115.

Tosoni A, Pitzalis S, Committeri G, Fattori P, Galletti C, Galati G. Resting-state connectivity and functional specialization in human medial parieto-occipital cortex. *Brain Struct Funct*. 2015:220(6):3307–3321.

Tovee MJ, Rolls ET, Azzopardi P. Translation invariance in the responses to faces of single neurons in the temporal visual cortical areas of the alert macaque. *J Neurophysiol*. 1994:72(3):1049–1060.

Treves A, Rolls ET. A computational analysis of the role of the hippocampus in memory. *Hippocampus*. 1994:4(3):374–391.

Treves A, Panzeri S, Rolls ET, Booth M, Wakeman EA. Firing rate distributions and efficiency of information transmission of inferior temporal cortex neurons to natural visual stimuli. *Neural Comput*. 1999:11(3):601–631.

Tsao D. The macaque face patch system: a window into object representation. *Cold Spring Harb Symp Quant Biol*. 2014:79:109–114.

Tsitsiklis M, Miller J, Qasim SE, Inman CS, Gross RE, Willie JT, Smith EH, Sheth SA, Schevon CA, Sperling MR, et al. Single-neuron representations of spatial targets in humans. *Curr Biol*. 2020:30(2):245–253.e4.

Ungerleider LG. Functional brain imaging studies of cortical mechanisms for memory. *Science*. 1995:270(5237):769–775.

Ungerleider LG, Haxby JV. 'What' and 'where' in the human brain. *Curr Opin Neurobiol*. 1994:4(2):157–165.

Valdes-Sosa PA, Roebroeck A, Daunizeau J, Friston K. Effective connectivity: influence, causality and biophysical modeling. *NeuroImage*. 2011:58(2):339–361.

Van Essen DC, Smith SM, Barch DM, Behrens TE, Yacoub E, Ugurbil K, Consortium WU-MH. The WU-Minn human connectome project: an overview. *NeuroImage*. 2013:80:62–79.

Van Essen DC, Glasser MF. Parcellating cerebral cortex: how invasive animal studies inform noninvasive mapmaking in humans. *Neuron*. 2018:99(4):640–663.

Van Hoesen GW. The parahippocampal gyrus. New observations regarding its cortical connections in the monkey. *Trends Neurosci*. 1982:5:345–350.

Vanni S, Hokkanen H, Werner F, Angelucci A. Anatomy and physiology of macaque visual cortical areas V1, V2, and V5/MT: bases for biologically realistic models. *Cereb Cortex*. 2020:30(6):3483–3517.

Vul E, Lashkari D, Hsieh PJ, Golland P, Kanwisher N. Data-driven functional clustering reveals dominance of face, place, and body selectivity in the ventral visual pathway. *J Neurophysiol*. 2012:108(8):2306–2322.

Wallis G, Rolls ET. Invariant face and object recognition in the visual system. *Prog Neurobiol*. 1997:51(2):167–194.

Weiner KS, Grill-Spector K. The evolution of face processing networks. *Trends Cogn Sci*. 2015:19(5):240–241.

Weiner KS, Barnett MA, Lorenz S, Caspers J, Stigliani A, Amunts K, Zilles K, Fischl B, Grill-Spector K. The cytoarchitecture of domain-specific regions in human high-level visual cortex. *Cereb Cortex*. 2017:27(1):146–161.

Wild B, Treue S. Primate extrastriate cortical area MST: a gateway between sensation and cognition. *J Neurophysiol*. 2021:125(5):1851–1882.

Wirth S, Baraduc P, Plante A, Pinede S, Duhamel JR. Gaze-informed, task-situated representation of space in primate hippocampus during virtual navigation. *PLoS Biol*. 2017:15(2):e2001045.

Wiskott L, Sejnowski TJ. Slow feature analysis: unsupervised learning of invariances. *Neural Comput*. 2002:14(4):715–770.

Wyss R, Konig P, Verschure PF. A model of the ventral visual system based on temporal stability and local memory. *PLoS Biol*. 2006:4(5):e120.

Yamins DL, Hong H, Cadieu CF, Solomon EA, Seibert D, DiCarlo JJ. Performance-optimized hierarchical models predict neural responses in higher visual cortex. *Proc Natl Acad Sci U S A*. 2014:111(23):8619–8624.

Yeatman JD, White AL. Reading: the confluence of vision and language. *Annu Rev Vis Sci*. 2021:7(1):487–517.

Yokoyama C, Autio JA, Ikeda T, Sallet J, Mars RB, Van Essen DC, Glasser MF, Sadato N, Hayashi T. Comparative connectomics of the primate social brain. *NeuroImage*. 2021:245:118693.

Zaharia AD, Goris RLT, Movshon JA, Simoncelli EP. Compound stimuli reveal the structure of visual motion selectivity in macaque MT neurons. *eNeuro*. 2019:6(6): ENEURO.0258-19.2019.

Zhuang C, Yan S, Nayebi A, Schrimpf M, Frank MC, DiCarlo JJ, Yamins DLK. Unsupervised neural network models of the ventral visual stream. *Proc Natl Acad Sci U S A*. 2021:118(3):e2014196118. https://doi.org/10.1073/pnas.2014196118.